ANL-82-81

SIDE-BY-SIDE COMPARISONS OF EVACUATED COMPOUND PARABOLIC CONCENTRATOR AND FLAT PLATE SOLAR COLLECTOR SYSTEMS

by

Arthur E. McGarity, John W. Allen,
and William W. Schertz

ARGONNE NATIONAL LABORATORY, ARGONNE, ILLINOIS

Operated by THE UNIVERSITY OF CHICAGO
for the U. S. DEPARTMENT OF ENERGY
under Contract W-31-109-Eng-38

DISCLAIMER

Printed in the United States of America
Available from
National Technical Information Service
U. S. Department of Commerce
5285 Port Royal Road
Springfield, VA 22161

NTIS price codes
Printed copy: A05
Microfiche copy: A01

Distribution Category:
Heating and Cooling--Active
Solar (UC-59a)

ANL-82-81

ANL--82-81

DE85 004833

ARGONNE NATIONAL LABORATORY
9700 South Cass Avenue
Argonne, Illinois 60439

SIDE-BY-SIDE COMPARISONS OF EVACUATED COMPOUND PARABOLIC CONCENTRATOR AND FLAT PLATE SOLAR COLLECTOR SYSTEMS

Arthur E. McGarity,* John W. Allen, and William W. Schertz

Energy and Environmental Systems Division
Solar Energy Section

October 1983

sponsored by

U.S. DEPARTMENT OF ENERGY
Office of the Assistant Secretary for
Conservation and Renewable Energy
Office of Solar Heat Technologies

*Department of Engineering, Swarthmore College, Swarthmore, Pennsylvania.

CONTENTS

CONTENTS (Cont'd)

FIGURES

FIGURES (Cont'd)

FIGURES (Cont'd)

TABLES

TABLES (Cont'd)

ACKNOWLEDGMENTS

The testing of three liquid-based solar heating systems for one year (and the validation of a computer model to simulate these systems) was sponsored by the U.S. Department of Energy (DOE), Office of Solar Heat Technologies. We are indebted to Gary Moore (formerly at DOE, Office of Solar Technology) for his support and encouragement in the early stages of the project and to John Goldsmith (DOE, Office of Solar Energy) in the later stages.

We extend our thanks to Kent Reed (now with the Solar Equipment Group, Center for Building Technology, National Bureau of Standards), the leader of this project at its beginning and a participant in decisions regarding the selection of the collectors and the testing scheme. We also express our gratitude to Robert Rush (formerly with the Argonne National Laboratory [ANL] Solar Applications Group) and Alvin Wantroba (Solar Applications Group), who took our ideas and simple drawings and built systems that worked well throughout the test period, and we thank Denise Voss and Ellen Bremner for their help in the preparation of this report.

SIDE-BY-SIDE COMPARISONS OF EVACUATED COMPOUND PARABOLIC CONCENTRATOR AND FLAT PLATE SOLAR COLLECTOR SYSTEMS

by

Arthur E. McGarity, John W. Allen, and William W. Schertz

SUMMARY

Three liquid-based solar heating systems employing different types of solar collectors were tested side by side at Argonne National Laboratory (latitude 42°N, longitude 88°W) near Chicago, Illinois, for one year (May 1981 - May 1982). The three systems were started each day with a storage temperature of 30°C, and no load was applied during the daylight hours. The 30°C starting storage temperature was chosen to allow ready comparison of the results with those from side-by-side tests of domestic-water-heating systems using flat plate collectors, performed at the National Bureau of Standards (NBS). The Argonne results have been extended through computer simulation to include operation at higher temperatures.

The three different types of collectors used in the tests at Argonne National Laboratory represented the 1980 state of the art in flat plate and compound parabolic concentrator (CPC) collector design. The three collectors used were as follows:

1) A flat plate collector with a black-chrome coated absorber plate and one low-iron glass cover;

2) An evacuated-tube CPC collector with a concentration ratio of 1.1, oriented with tubes and troughs along a north-south (N-S) axis; and

3) An evacuated-tube CPC collector with a concentration ratio of 1.3 and one low-iron glass cover, with tubes and troughs oriented along an east-west (E-W) axis.

Analysis of the test results indicates that, among these collectors, the flat plate collector system was the most efficient during warm weather. The CPC collector systems were slightly more efficient than the flat plate collector system during cold weather. The CPC collector systems operated (i.e., they delivered useful energy to storage) more frequently than the flat plate collector system during all seasons of the year. Usually, when all three systems were operating, the flat plate system was most efficient. However, the CPC systems operated under cold and hazy-sky conditions that were too adverse for flat plate collector operation. During the tests, the CPC systems operated for some portion of almost every day that they were not covered with snow.

Regression analysis was used to extract information about system parameters from the tests to help explain the results. We obtained "system parameters" related to the collectors' optical efficiencies and heat-loss coefficients and to the effects of the

diffuse solar-radiation fraction and the wind speed on collector performance. These parameters may be useful in the development of testing and rating methods for solar heating systems.

The computer simulation model ANSIM was validated by means of data from the side-by-side tests. The ANSIM model, which uses analytical solutions to the storage energy balance, was coupled to a CPC ray-tracing program to allow simulation of CPC system performance. This report contains comparisons of ANSIM with the general simulation program TRNSYS. The ANSIM model produces results that are identical to those of TRNSYS, but ANSIM requires significantly less computing time. The validated ANSIM model was used to predict the performance of the CPC and flat plate collector systems over several different years, at three geographical locations, for a variety of operating-temperature ranges and collector-design improvements.

Simulated side-by-side tests of 1983 state-of-the art collectors are especially relevant, because such tests predict how the comparisons would differ if collectors incorporating the latest advances in CPC design were used in the tests. Such collectors are now commercially available. In 1983, improved absorber tubes having an absorptance of about 0.95 became available; this represents a significant improvement over the tubes produced in 1980, which had an absorptance of about 0.8. The effects of this improvement have been estimated using ANSIM. Figures 5.3 and 5.7 in this report (reproduced in this summary as Figures S.1 and S.2) allow comparisons of the 1980 and 1983 state-of-the-art collectors in simulated systems operated with a daily starting temperature of 30°C. We see that the performance of the CPC collector systems improved substantially relative to that of the flat plate collector system. The CPC systems performed substantially better than did the flat plate system during the cold months and about the same as the flat plate system during the warm months.

Typically, CPC collectors are used in applications requiring operation at temperatures significantly higher than the 30-60°C range that resulted from the daily starting temperature of 30°C used in the tests. Therefore, we have generated simulated side-by-side comparisons covering operation at higher temperatures. Figure 5.8 (reproduced here as Figure S.3) shows simulated comparisons of systems using 1983 state-of-the-art collectors operated with a daily starting storage temperature of 75°C. At this temperature, the improved CPC collectors performed significantly better than the flat plate collector throughout the year. For all three systems, average daily gains were less with the 75°C starting temperature than with the 30°C starting temperature. However, the flat plate system's performance decreased much more than the performance of either CPC system, because the CPC collectors had heat-loss coefficients that were very low compared with that for the flat plate collector. Figure 5.9 (reproduced here as Figure S.4) shows simulated comparisons of systems using 1983 state-of-the-art collectors operated with a daily operating temperature of 120°C, which would be typical of a steam-generating system. During four months of the year, the flat plate system did not operate at all. The E-W CPC collector had the best performance in this temperature range, because its heat-loss coefficient was lower than that of the N-S CPC (due to the higher concentration ratio of the E-W CPC).

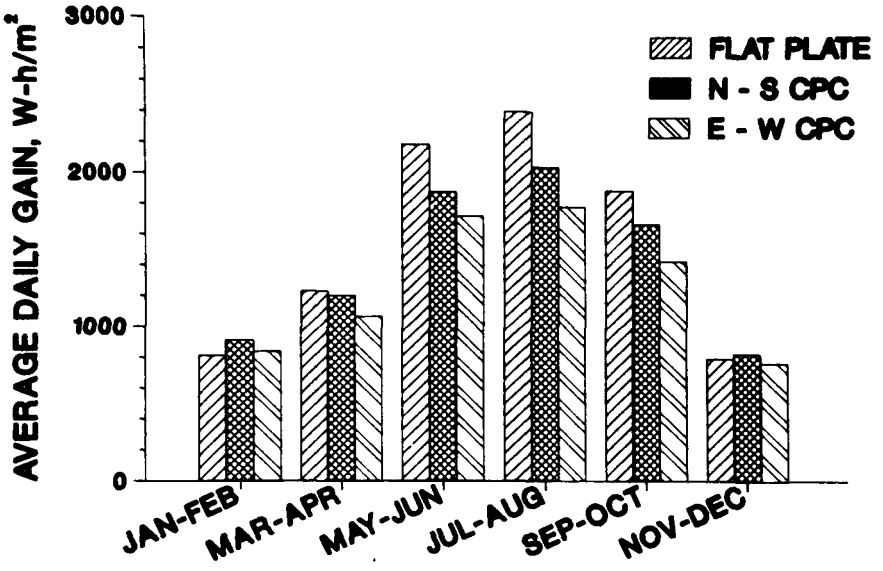

FIGURE S.1 Simulated Collector Performance at ANL, Based on 1980 Weather Data (Daily starting temperature of storage is 30°C.)

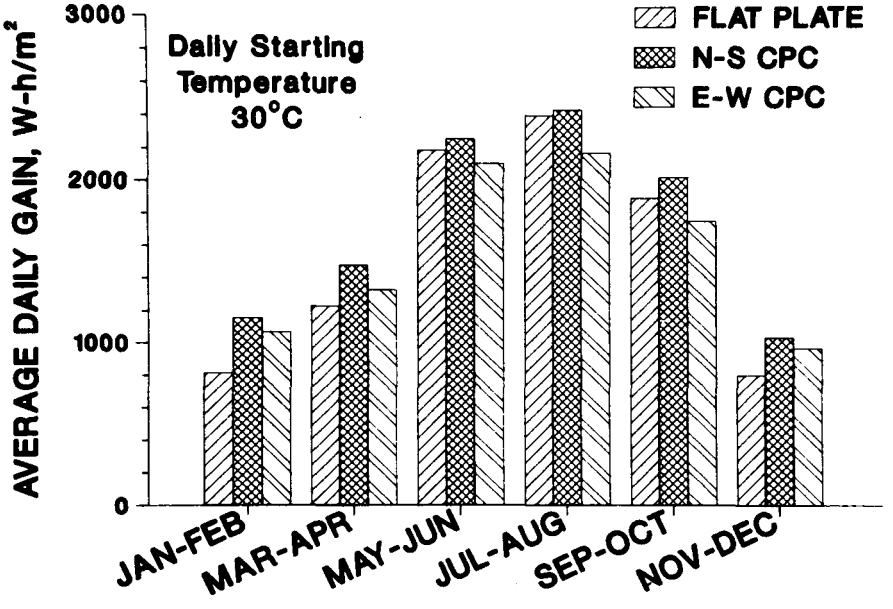

FIGURE S.2 Simulated System Performance at Low Temperature Using 1983 State-of-the-Art Collectors (The N-S CPC and E-W CPC systems use new, improved absorber tubes, absorptance = 0.95. Daily starting temperature of storage is 30°C. Based on 1980 ANL weather data.)

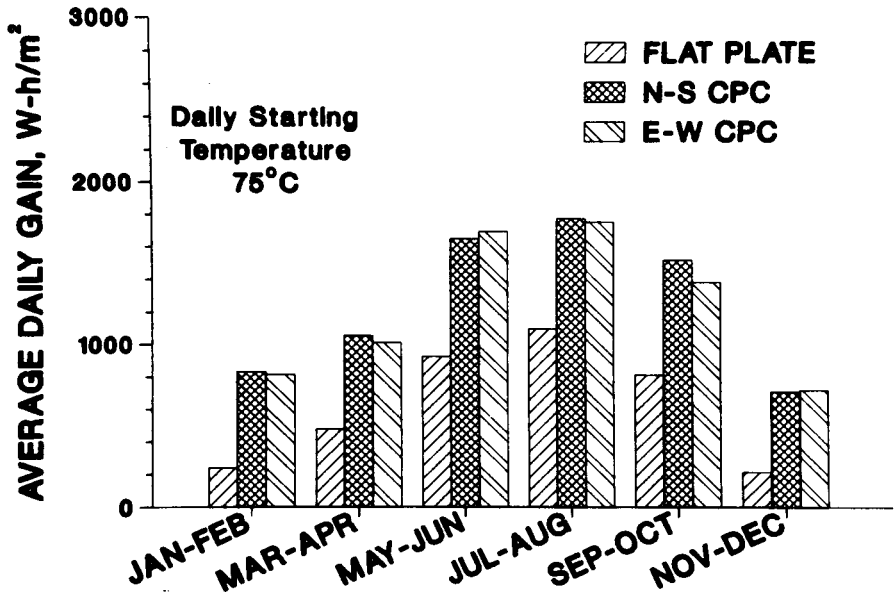

FIGURE S.3 Simulated System Performance at Higher Temperature Using 1983 State-of-the-Art Collectors (The N-S CPC and E-W CPC systems use new, improved absorber tubes, absorptance = 0.95. Daily starting temperature of storage is 75°C. Based on 1980 ANL weather data.)

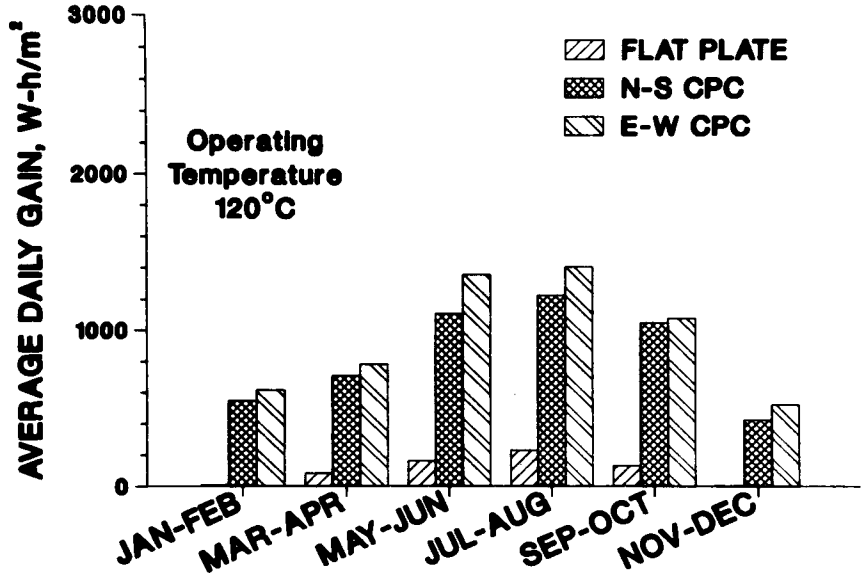

FIGURE S.4 Simulated System Performance at Steam-Generating Temperature Using 1983 State-of-the-Art Collectors (The N-S CPC and E-W CPC systems use new, improved absorber tubes, absorptance = 0.95. Collector operating temperature is a constant 120°C. Based on 1980 ANL weather data.)

Page(s) Missing

from

Original Document

1 INTRODUCTION

A solar collector using evacuated tubes and compound parabolic concentrators (CPCs) has performance characteristics that differ in many ways from those of a common flat plate collector. One difference is that the use of evacuated tubes causes CPC collectors to have much lower heat losses than do flat plate collectors. Another difference is that the CPC collector's optical efficiency has a strong and complex dependence on the angle of incidence of the solar radiation.[1,2]

This report presents results of experimental comparisons of three different types of collectors in heating systems operated side by side for more than a year at Argonne National Laboratory (ANL), together with results of simulated comparisons for ANL and other locations. Two of the systems used CPC collectors, and the third system used a well-made flat plate collector. These collectors represented the state of the art in flat plate and CPC collector design as of 1980. All three collector arrays faced south and were tilted at an angle of 42° with respect to the horizontal (to match the 42°N latitude at ANL). The collectors were mounted in fixed positions. They did not track the sun, and their tilt angles were not seasonally adjusted.

The first CPC collector used a concentrator with an acceptance angle of 110°, a concentration ratio of 1.1, and a north-south (N-S) orientation of the tube axes. (By "north-south orientation," we mean that if the collector were horizontal, the absorber tubes and concentrator troughs would be aligned north-south.) With an N-S orientation, the *daily* motion of the sun is transverse to the tube and trough axes. Thus, the wide acceptance angle was necessary to avoid the need for tracking. This collector, hereafter referred to as the "N-S CPC," has no cover glass over the concentrator troughs.

The second CPC collector had an acceptance angle of 72°, a concentration ratio of 1.34, and an east-west (E-W) orientation of the tube axes. (By "east-west orientation," we mean that the absorber tubes and concentrator troughs are aligned east-west.) With an E-W orientation, the *seasonal* motion of the sun is transverse to the trough axes. Thus, compared with the N-S CPC, the second collector's acceptance angle was smaller and the concentration ratio higher, because the variations in the transverse incidence angle (±23° for solar noon) for the second collector were less than the daily variations in transverse incidence angle (±90°) for the N-S CPC. The E-W CPC had a single cover glass over the concentrator troughs to prevent accumulation of dust, snow, and ice in the troughs.

The third collector was a single-glazed, black-chrome-plated flat plate collector. All three collectors were purchased in the fall of 1980.

1.1 NEED FOR SIDE-BY-SIDE TESTS

The understanding of performance characteristics of CPC collectors has developed to the point that manufacturers are now producing several different models. All of the collectors used in this study were commercially manufactured. However, methods of testing and rating the performance of CPC collectors and the systems in which they are installed continue to be an important area for investigation.

Existing system-performance evaluation methods have been developed with an emphasis on flat plate systems. These methods include analytical methods, such as f-Chart[3], and short-term experimental testing procedures, such as the American Society of Heating, Refrigeration, and Air-Conditioning Engineers (ASHRAE) Standard 95-1981[4] and the relative solar rating method of Chandra and Khattar[5]. At present, long-term side-by-side tests are necessary for comparisons of different CPC collector systems. Such tests are also needed in order to obtain long-term performance results that are necessary to examine the usefulness of analytical and short-term experimental rating methods for these systems.

1.2 SELECTION OF OPERATING CONDITIONS

One aspect of side-by-side testing that complicates the design of experiments is the selection of an operating-temperature range for the systems. Flat plate collectors are used primarily in low-temperature applications, whereas evacuated CPC collectors are used primarily in moderate-to-high-temperature applications. Ideally, long-term tests should be conducted at several different operating temperatures. One method of performing such tests would be to operate each collector at the temperature that optimizes its performance; however, the results of such tests would be difficult to compare. Therefore, it is desirable to select a single operating-temperature range for all three systems.

For our long-term tests, we chose a daily starting temperature of 30°C for the storage tank in each of the three systems. The systems were operated with no load during the day. Thus, it was possible to determine the daily energy gain of a system from simple measurements of the daily increase in storage-tank temperature. Under the chosen operating conditions, the storage-tank temperatures were almost always in the 30-60°C range, which corresponds to domestic-water-heating temperatures. We chose this temperature range so that our results could be compared with the results of side-by-side tests of six different domestic-water-heating systems conducted at the National Bureau of Standards (NBS).[6] We obtained predictions of the performance of the ANL systems at higher temperatures by running computer simulation models that were validated using the results from our low-temperature tests.

1.3 SIMULATION MODELING AND VALIDATION

The trends observed in side-by-side testing in this study have been extended through computer simulation of the three different systems. Measured results from the test systems were compared with simulated results to validate the computer simulations. The simulation model was then employed to create simulated side-by-side comparisons, which were used to examine changes in relative performance resulting from using weather data for different years and climates, from the use of different operating temperatures, and from improvements in collector design.

The optical performance of the CPC collectors was modeled by a ray-tracing program developed at ANL for collector-design studies.[7] The ray-tracing program was coupled to a thermal simulation model, ANSIM[8]. The ANSIM model was used because its

use of analytical solutions to the governing equations substantially reduced the computing expense.

1.4 CONTENTS OF THIS REPORT

In Chapter 2, the side-by-side tests are described. Details of the systems, their operation, and the instrumentation used to monitor performance are presented.

Chapter 3 presents comparisons of the measured performances of the three systems. Differences in average daily performance for each season of the year are explained in terms of performance characteristics, including the amount of time each system operated and the average efficiencies of the systems while they were operating. System parameters derived from multivariate regression analyses of the performance data are also presented. Effects of snow and ice are discussed, and results from a period of operation at higher temperatures are presented.

Chapter 4 presents validations of the computer simulation model, including day-by-day comparisons of measured and simulated performances for periods in both summer and winter.

Chapter 5 presents simulated side-by-side comparisons. These comparisons include the following: (1) operation of the three test systems using three different years of weather data at ANL to determine how well the 1981-82 comparisons represented long-term performance comparisons, (2) operation of the three test systems in different climates, (3) modifications to the design of the E-W CPC collector, (4) use of 1983 state-of-the-art collector designs at different temperatures for the three systems, (5) improvements in the design of the CPC collectors, and (6) operation of the three test systems at steam-generating temperatures.

Finally, Chapter 6 discusses the implications these tests have for the validity of various methods of system testing and evaluation. Suggestions are made for future research on methods of combining short-term system tests with simulation modeling in order to develop a method of rating solar energy systems.

2 DESCRIPTION OF SIDE-BY-SIDE TESTS

2.1 DESCRIPTION OF SYSTEMS

The side-by-side comparison consisted of long-term testing of three different solar heating systems at ANL (Argonne, Illinois -- latitude 42°N, longitude 88°W). All three systems were identical except for collectors and solar controllers. Each system consisted of a collector array, a 120-gal storage tank containing 92 gal of a 50/50 ethylene-glycol/water mixture, a solar controller, a pump, visual and electrically readable flowmeters, a temperature switch, and some electrically operated valves. The lengths of the piping runs were all nominally the same. The flat plate system and the E-W CPC system employed the same solar controller, which used a 9°F temperature difference between storage and collector outlet to start the solar collector pump and a 5°F temperature difference to stop it. The N-S CPC system required a different type of solar controller, because it was a drain-down collector; the collector outlet could not be used for the temperature-difference measurement. Instead, the method used for the N-S CPC solar controller was to start the solar collector pump when the temperature in the collector reached 180°F and to stop the flow when the temperature difference between storage and collector outlet was 5°F. A mode-control panel set the system in the collection mode during the day and in the drain, mix, and heat-dump modes during the night (see Section 2.2).

Table 2.1 gives collector manufacturer names, models, and sizes. For the flat plate and N-S CPC systems, the number of collectors used was as recommended by the manufacturer for a typical residential solar domestic-hot-water (DHW) heating system. The E-W CPC was not recommended for DHW applications, because it was designed for higher-temperature operation.

TABLE 2.1 Collector Arrays

Collector Type	Manufacturer	Model	Number of Collectors	Total Active Area (m^2[ft^2])
N-S CPC	Sunmaster Corporation	DEC-8	3	3.9 [42]
E-W CPC	Energy Design Corporation	XE-300	2	5.2 [56]
Flat Plate	Energy Design Corporation	HP-150	2	4.45 [48]

Figure 2.1 shows manufacturer-supplied efficiency curves for the three collectors. All collectors were tested at DSET Laboratories, Inc., Phoenix, Arizona.

Figure 2.2 shows the transverse incidence-angle modifiers for the two CPC collectors. Transverse movement was across the trough rather than longitudinal (parallel) to the trough. As the sun moved from east to west daily, it moved transversely with respect to the N-S CPC trough. The N-S CPC had an acceptance angle of $\pm$ 55° to allow it to collect solar energy within the acceptance angle for at least seven hours each day. For the E-W CPC, the sun moved transversely with respect to the trough as it moved seasonally from north to south and back. The E-W CPC had an acceptance angle of ±35°, which allowed it to collect solar energy within the acceptance angle for at least seven hours each day. The incidence angle modifiers for both CPCs increased with transverse incidence angle out to near the acceptance angle. The incidence-angle modifiers did not drop immediately to zero outside the acceptance angle, especially in the case of the N-S CPC. The incidence-angle modifier of the flat plate collector is also shown in Figure 2.2. The optical performance of the flat plate collector was omnidirectional, so it was not necessary to distinguish between north-to-south and east-to-west movements. The longitudinal incidence-angle modifiers for both CPCs were similar to the incidence-angle modifier of the flat plate collector.

Figure 2.3 is a photograph of the three collector arrays, showing the N-S CPC array on the left, the flat plate array in the middle, and the E-W CPC array on the right. All three systems faced due south and were tilted at 42° with respect to the horizon.

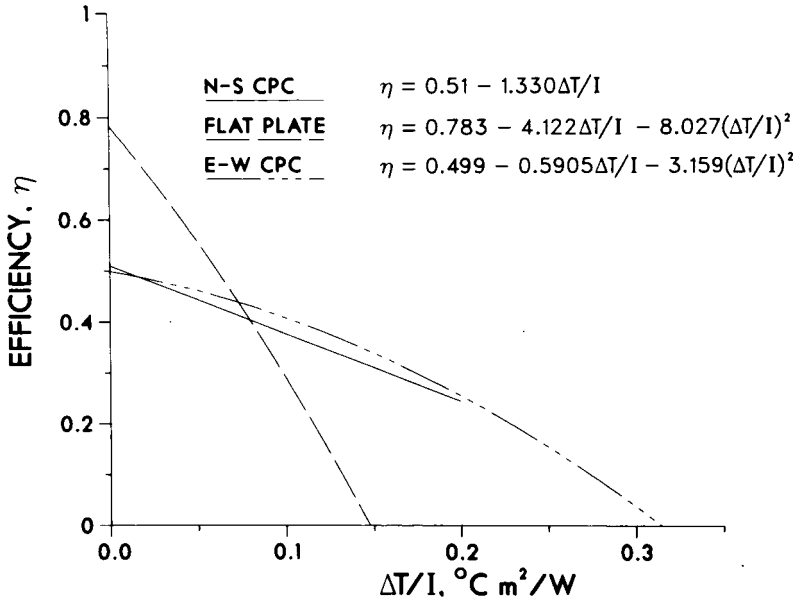

FIGURE 2.1 Collector Efficiency Curves (ΔT is the collector-inlet temperature minus the ambient temperature, and I is the global insolation on the collector surface.)

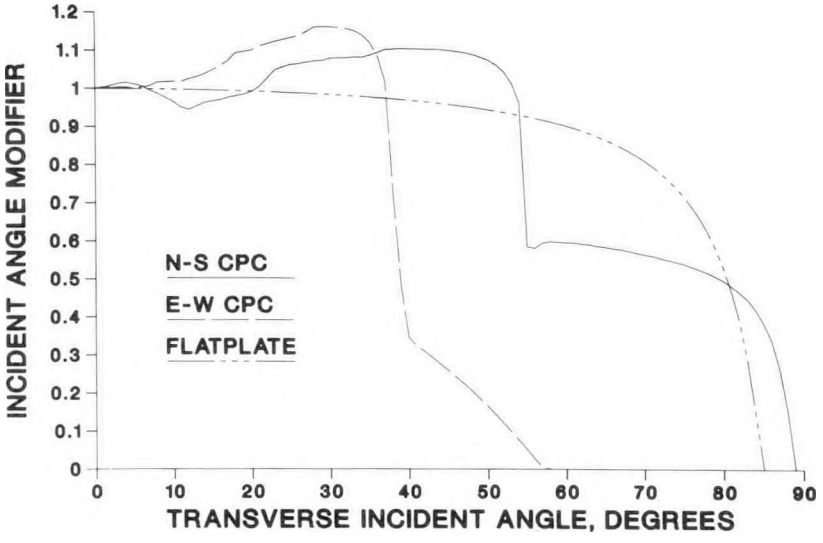

FIGURE 2.2 Transverse Incidence-Angle Modifiers

FIGURE 2.3 Collector Test Stand, Showing the Three Collector Arrays
(The building in the foreground contains the pumps and storage tanks. The system on the left is the N-S CPC, the system in the center is the flat plate, and the system on the right is the E-W CPC. The E-W CPC does not appear black, because the photograph was taken from outside the acceptance angle of the collector.)

Figure 2.4 is a piping diagram of the N-S CPC system. The flat plate and E-W CPC systems were not drain-down designs and did not have the zone heating valve, ZV4.* The E-W CPC had two pumps in series because of higher piping resistances. Figure 2.5 shows the flat plate system's pump control box, which contained the pump, the valves, the temperature switch, and the flowmeters. The heat exchangers were located outside the building that housed the tanks and the plumbing control boxes. Table 2.2 lists the collector-system components.

2.2 OPERATION OF SYSTEMS

The piping diagram of the N-S CPC, Figure 2.4, shows the location of the valves and pumps named in the description of the system's four operating modes. The four modes were as follows:

1) *Collection Mode.* From 07:00 to 21:00, ZV1* was open and each system was controlled by its own solar controller, with no load imposed. The solar controllers used the temperature difference between the collector and the storage to determine when the collector should operate.

2) *Drain Mode (N-S CPC only).* From 21:00 to 21:30, the pump was off and ZV4 in the N-S CPC system was open to connect the collectors directly to the storage tank to guarantee that the ethylene-glycol/water fluid would drain from the collectors.

3) *Mix Mode.* From 21:30 to 23:00, ZV2 was open and the pump was on to mix the tank contents. Mixing was completed in less than ten minutes.

4) *Dump Mode.* From 23:00 to 07:00, the pump was on and the temperature switch was activated. When the temperature rose above the set point (usually 30°C), the temperature switch powered ZV3 in order to dump heat by passing the solution through the heat exchanger. When the temperature fell below the set point, the temperature switch powered ZV2 so that the solution would bypass the heat exchanger. The pump ran until 07:00 to keep the tank contents mixed.

Figure 2.6 is a photograph of the mode-control panel, which selected the mode of operation and contained the solar controllers. This panel was controlled by a multipoint timer that operated a stepping relay to switch from mode to mode. In the morning a second timer reset the stepping relay to restart the cycle.

---

*The "ZV" in ZV4, ZV1, etc. signifies "zone heating valve."

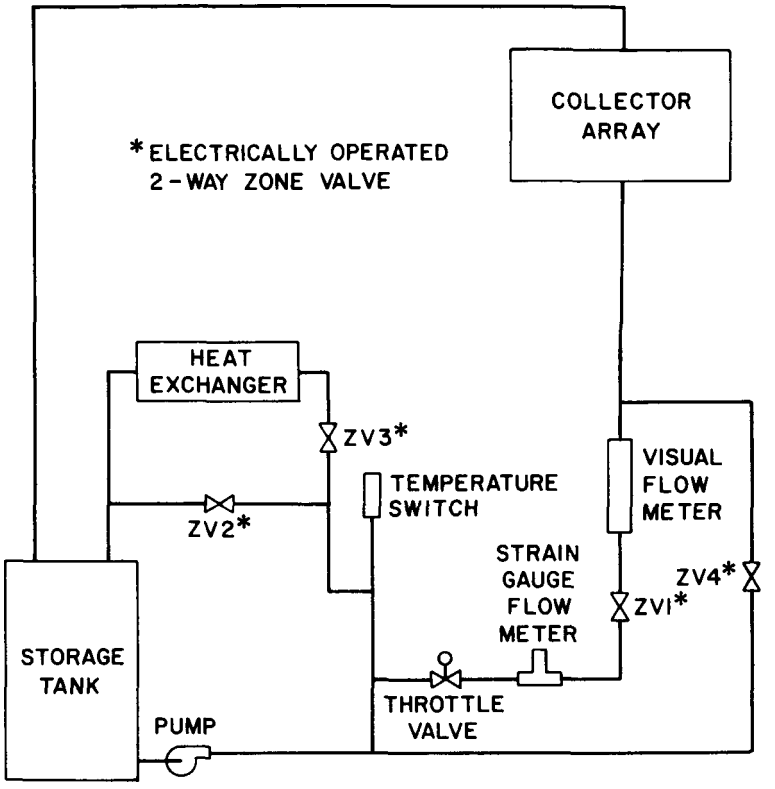

FIGURE 2.4 Piping Diagram of the N-S CPC System

2.3 INSTRUMENTATION

The data-acquisition system was a Kaye Instruments Digistrip III. Table 2.3 briefly lists the items of information recorded each hour. The Digistrip III accumulated data calculated at 6-s intervals to determine average wind speed, total hourly insolation, total daily insolation, and pump run time for each hour.

The wind speed was measured with a Weathermeasure Corporation Model W101-DC/AC Skyvane I Wind System. The output from this instrument was accumulated by the Digistrip III to determine average wind speed. The horizontal and tilted pyranometers were both Eppley Precision Spectral Pyranometers (PSPs).

The output of the Digistrip III was recorded on paper and on cassette tape using an MFE Corporation Model 2500 Buffered Data Terminal. The MFE 2500 was later connected between a video terminal and a DEC VAX 11-780 computer to allow the data to be transferred to a computer file. All data reduction was done on the computer.

All temperatures were measured using Type T thermocouples. The Digistrip III converted the millivolt outputs of the thermocouples to temperatures.

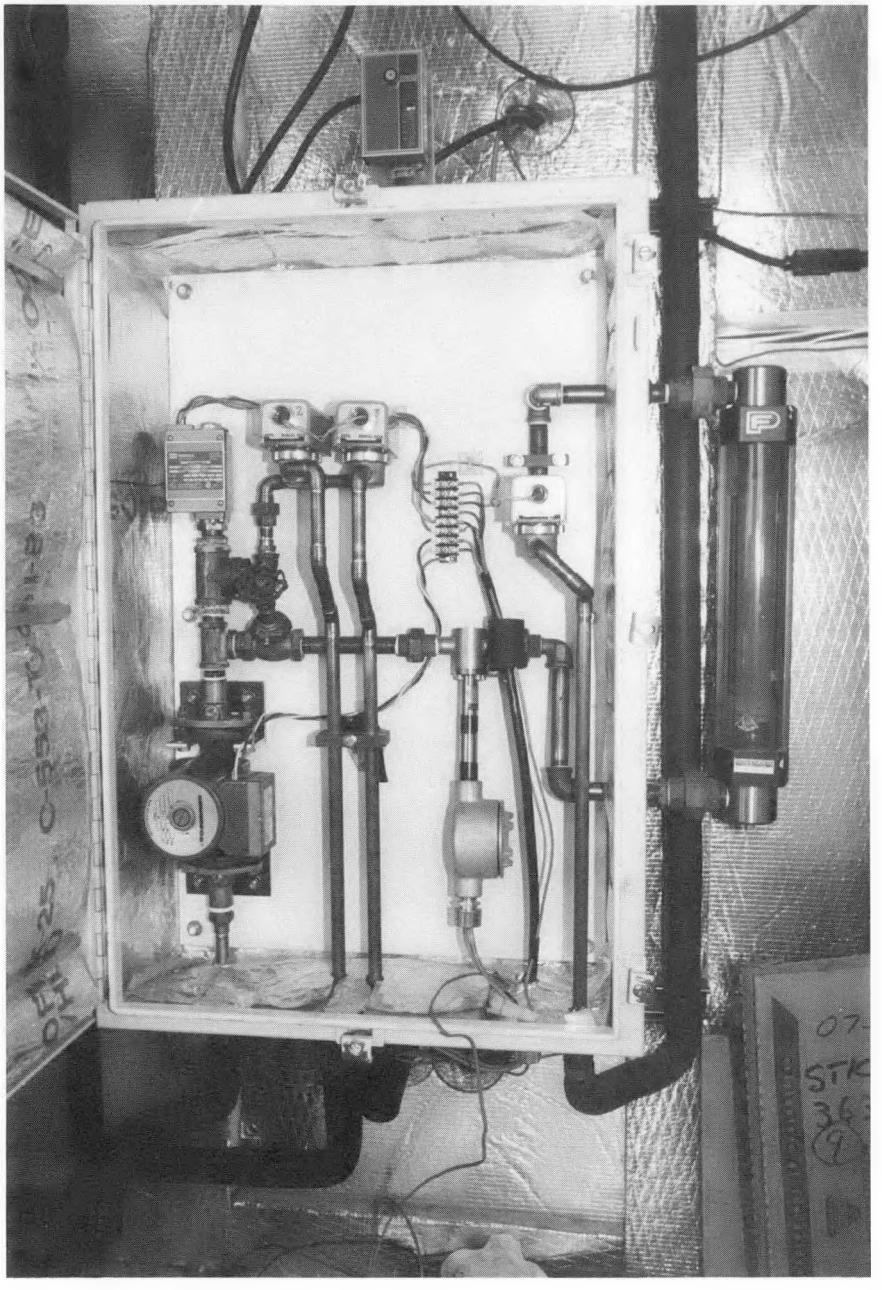

FIGURE 2.5 Pump Control Box for the Flat Plate System

TABLE 2.2 Components of the Collector Systems

Component	Manufacturer	Model Number
Storage Tank	A. O. Smith	SEH-120
Zone Valve	White-Rogers	Series 13A01
Temperature Switch	Delaval	ML1H-H 203W
Pump	Grundfos	UP265-64F
Heat Exchanger	Singer	LPC-50
Visual Flowmeter	Fischer and Porter	3565-760
Strain Gauge Flowmeter	Ramapo	Mark V-1/2-J-02
Solar Controller		
Flat Plate and E-W CPC	Independent Energy	C30
N-S CPC	Sunmaster Corporation	SPC-80

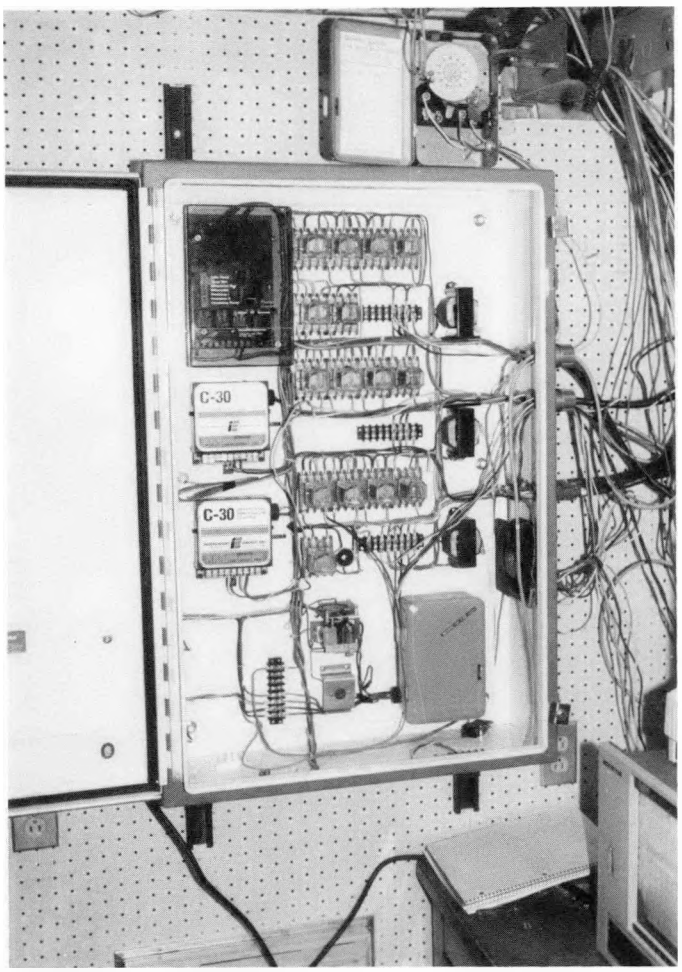

FIGURE 2.6 Mode-Control Panel

TABLE 2.3 Data Recorded Hourly in System Tests

Property	Environmental Data Recorded	Data Recorded for Each Collector
Wind	Average Speed Instantaneous Direction	
Insolation	Instantaneous Value[a] Hourly Total[a] Daily Total[a]	
Temperature	Outdoor Ambient Storage-Tank Building	Collector In Collector Out Storage In Storage Out
Fluid Flow		Bridge Output Flow Rate Pump Run Time

[a]Measured both by horizontal pyranometer and by tilted pyranometer.

3 RESULTS FROM SIDE-BY-SIDE TESTS

In this chapter, we present results obtained by monitoring the performance of each system from May 1981 until June 1982. Results from higher-temperature tests during late June and early July of 1982 are also presented.

Table 3.1 indicates the number of days during each month for which useful data were collected. Some months have missing days because of problems with equipment start-up (during May and June of 1981), instrument failures, and snow cover on the collectors. The tanks were operated outside of any enclosure during the summer months. The systems were not operated in September and October of 1981; during that period a heated enclosure was built to provide the tanks with a warm, dry environment.

TABLE 3.1 Number of Days of Useful Data Collection between May 1981 and May 1982

Period	Number of Useful Days	Number of Useful Days with Collector Operation: Flat Plate	N-S CPC	E-W CPC
Entire Period	199	182	191	195
Summer	64	64	64	64
May	7	7	7	7
June[a]	14	14	14	14
July	28	28	28	28
August	15	15	15	15
Winter	67	54	64	64
November	9	6	8	8
December	21	17	20	20
January	15	12	14	15
February	22	19	22	22
Spring	68	64	63	67
March	23	20	22	22
April	29	28	25	29
May	16	16	16	16

[a]The June data include days with operation at higher than normal temperatures due to a malfunction that defeated the heat-dump mode on all three systems.

After most snowfalls, the snow was removed by hand from all three collectors. However, on a few occasions the snow was left until it melted so that the performance of snow-covered collectors could be observed. Snow and ice effects are discussed in Section 3.4. For the present analysis, all days on which the collectors were partially or completely covered with snow or ice have been removed from the data.

The resulting data are examined in different ways. First, average daily performances during three "seasons" are compared in terms of average daily gains per unit collector area and average daily efficiencies. (The "seasons" are defined as follows: "Summer" consists of May through August of 1981; "Winter" consists of November and December of 1981 and January and February of 1982; "Spring" consists of March through May of 1982.) Next, results on the average fraction of each day that the collectors operated (run-time fraction) are compared, and the average system efficiencies while the collectors were in operation are presented. Experimental system parameters derived from multivariate regression analyses are presented to provide additional insight into the differences among the three systems. Effects of snow and ice are discussed, and the results from the period of higher-temperature operation are presented.

3.1 AVERAGE DAILY RESULTS

Figure 3.1 presents comparisons of the seasonal average daily energy gains per square meter of collector area for each of the three systems. To determine the average daily gains, each day at 07:00 and 22:00 (local time) the storage tanks were mixed to create a uniform temperature, and the temperatures were measured. The difference between the 22:00 and 07:00 temperatures was multiplied by the mass and specific heat of the storage liquid to determine the energy gain in watt-hours. The gain of each system was divided by the system's collector area, and averages were taken for each season and over the entire year.

The relative performance of the three systems varied considerably from season to season. During the summer, optical performance characteristics were especially important, because thermal losses were low. The flat plate collector, with its superior optical efficiency, was the best performer. The performance of the two CPCs, with their lower optical efficiencies, was not so good as that of the flat plate collector.

During the winter, thermal losses were greater because of the much lower outdoor ambient temperatures. The low thermal losses of the CPC collectors (with their evacuated-tube absorbers) resulted in slightly better winter performance than that of the flat plate system. The relatively high concentration of the E-W CPC further reduced thermal losses and resulted in winter performance almost as good as that of the N-S CPC. In fact, during January, the E-W CPC system performed slightly better than the N-S CPC system, because the higher optical losses of the E-W CPC, which were due to the cover glass, were more than offset by the EW-CPC's lower thermal losses.

Figure 3.2 presents comparisons of average daily system efficiencies. The daily system efficiency was calculated by dividing the daily gain by the total amount of solar radiation incident on the plane of the collector during the day. Comparisons of daily system efficiencies are similar to comparisons of daily gain. The efficiency of the E-W

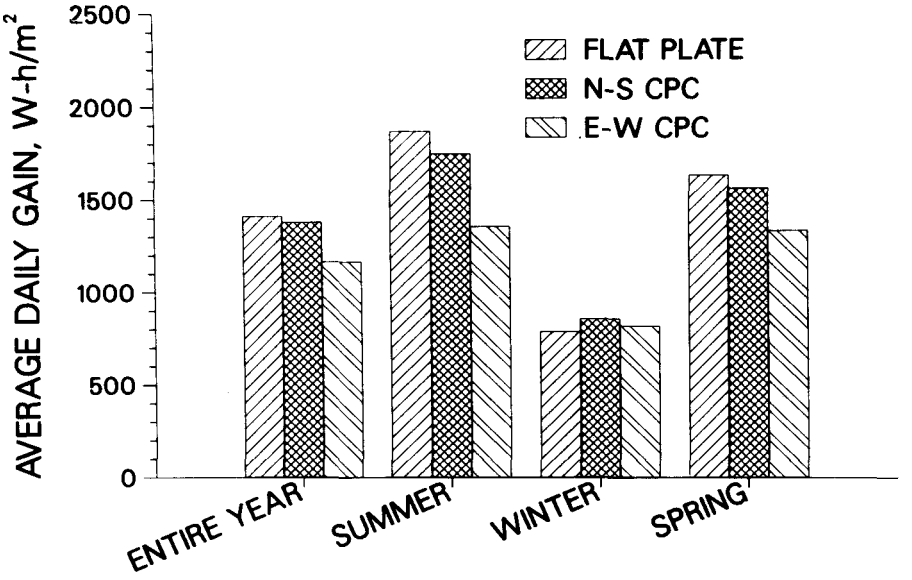

FIGURE 3.1 Seasonal Average Daily Energy Gains (Daily starting temperature of storage is 30°C.)

CPC system did not vary greatly between seasons (because of its low thermal-loss and wind-effect coefficients; see Section 3.3), whereas the other two systems showed substantial seasonal variations.

3.2 SYSTEM RUN-TIME RESULTS

Another approach to understanding the differences between the three systems is to examine system efficiencies based only on the periods of time that the collectors operated. Figure 3.3 presents run-time fractions, and Figure 3.4 presents run-time efficiencies, for each system during each season. The run-time fraction for each season is the amount of time that the collector operated, divided by the total time that the sun could have shone (under clear-sky conditions) on the plane of the collectors. The run-time efficiency for each season is the sum of the daily gains divided by the total insolation on the collector array while the collector operated.

The CPC systems operated a greater fraction of the time than did the flat plate system during every season. Over the year, the N-S CPC operated most frequently in the summer, but the E-W CPC operated most frequently in the winter and with the same frequency as the N-S CPC during the spring.

The run-time efficiencies show that on the average, when all three systems were running with 30°C starting temperatures, the flat plate system was the most efficient. However, the higher run-time fractions of the CPC systems indicate that they could operate during the marginal periods of low insolation and low outdoor temperature. The additional energy collected during marginal periods accounts for the superior performance of the CPCs during the winter.

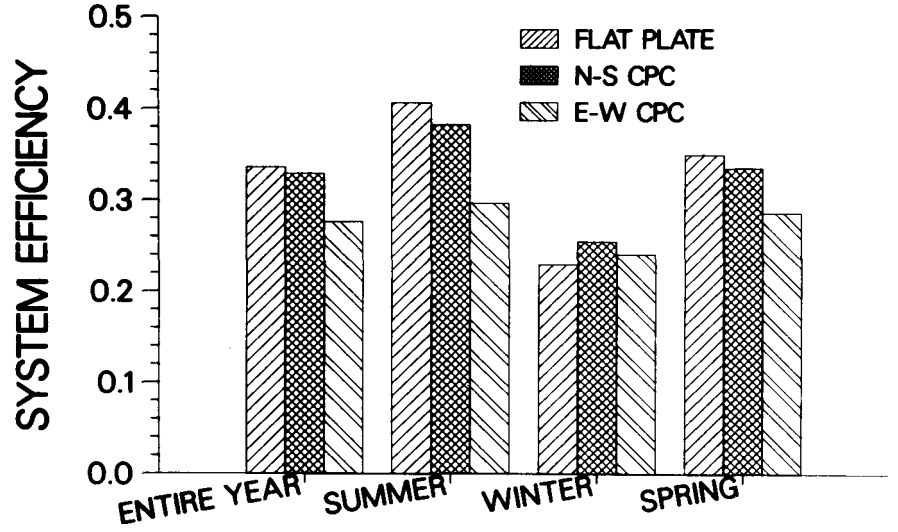

FIGURE 3.2 Average Daily System Efficiencies (Daily starting temperature of storage is 30°C.)

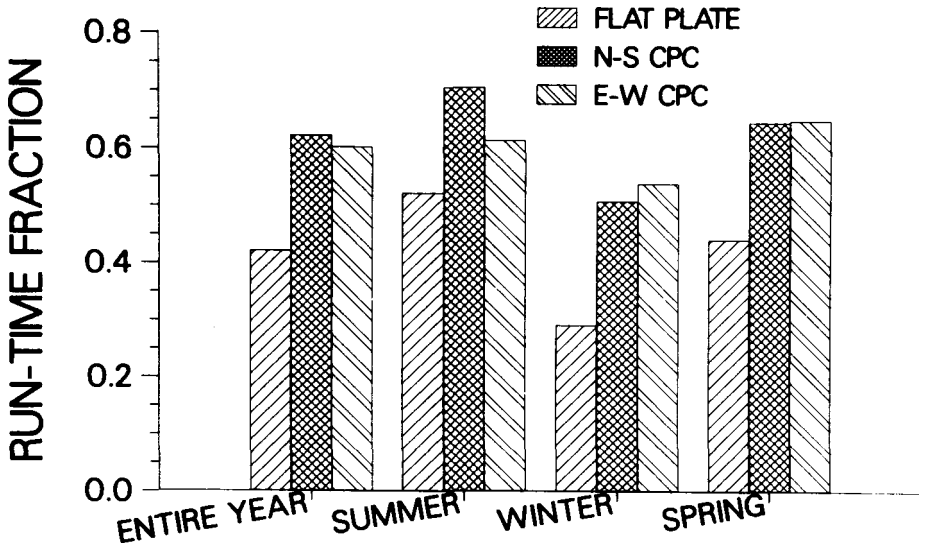

FIGURE 3.3 Run-Time Fractions (Daily starting temperature of storage is 30°C.)

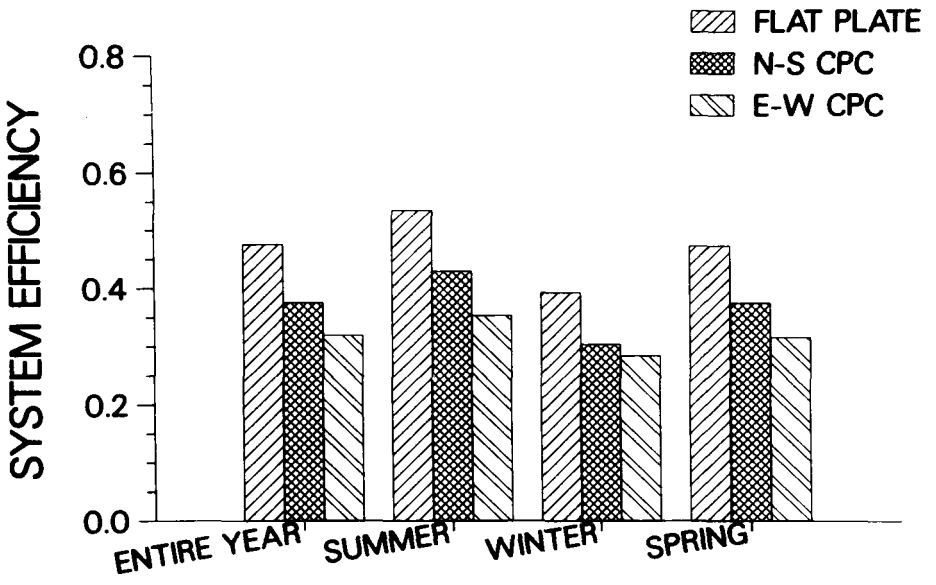

FIGURE 3.4 Run-Time Efficiencies (Daily starting temperature of storage is 30°C.)

3.3 SYSTEM PARAMETERS

We now present results of regression analyses to provide additional insight into the significance of the test results. The regression analyses also yield a set of parameters for comparing different systems that reveals the effects of differences in system-control strategies and run-time fractions.

The theoretical basis for the regressions was a linear model of the system, similar to the Hottel-Whillier-Bliss equation commonly used to model solar collectors. We applied the model to both run-time and daily average data.

The model accounts for optical gains with the optical efficiency, η, and for thermal losses with the loss coefficient, U. The model also accounts for the effect that the daily diffuse fraction, D, has upon η. The daily diffuse fraction is equal to the daily diffuse solar radiation divided by the daily total solar radiation. Direct measurements of the diffuse radiation were not available, so D was estimated by applying the regression formula developed by Boes et al.[9] to hourly measurements of global horizontal radiation to determine hemispherical sky radiation, which was assumed to be isotropic. Ground-reflected radiation was also estimated. Total diffuse radiation was calculated as a weighted sum of the sky and the ground components, where the "weights" were geometrical factors that depended on the collector tilt angle. The diffuse sky coefficient, a_D, is a measure of the effect of diffuse radiation on system performance. Finally, the model also accounts for the effect that the wind speed, W, has upon U. The wind coefficient, a_W, is a measure of the increase in system heat loss due to wind.

Equations 1, 2, and 3 present the model:

$$Q_{day} = \eta I - U[A(T-T_a)t] \qquad (1)$$

$$\eta = \eta' - a_D D \tag{2}$$

$$U = U' + a_W W \tag{3}$$

where:

Q_{day} = daily gain ($W \cdot h \cdot day^{-1}$)

η = optical efficiency

I = insolation ($W \cdot h \cdot day^{-1}$)

U = loss coefficient ($W \cdot °C^{-1} \cdot m^{-2}$)

A = collector area (m^2)

T = average storage temperature (°C)

T_a = average outdoor temperature (°C)

t = time, either daylight or run-time period (hours)

η' = clear-sky optical efficiency

a_D = diffuse-sky coefficient

D = diffuse fraction (defined in text above)

U' = calm-air loss coefficient ($W \cdot °C^{-1} \cdot m^{-2}$)

a_W = wind coefficient [$(W \cdot °C^{-1} \cdot m^{-2})/(m \cdot s^{-1})$]

W = wind speed ($m \cdot s^{-1}$)

When the model was applied to run-time data, only the periods that the collector operated were included in the daily insolation totals and in the daily temperature averages. On the other hand, when the model was applied to entire-day data, the insolation totals and temperature averages were taken for the entire time the sun could have shone on the collector each day. The daily gain, Q_{day}, is the same in both cases and is based on daily storage-energy gain.

The run-time coefficients η', U', a_D, and a_W were obtained through multivariate linear regression analysis of 131 days of useful data from summer and winter. Run-time coefficients for each system are presented in Figures 3.5, 3.6, and 3.7.

Figure 3.5 presents run-time optical-efficiency parameters for the systems and compares these system parameters with corresponding parameters for the collector alone. The coefficient a_D was found to be significantly different from zero only for the

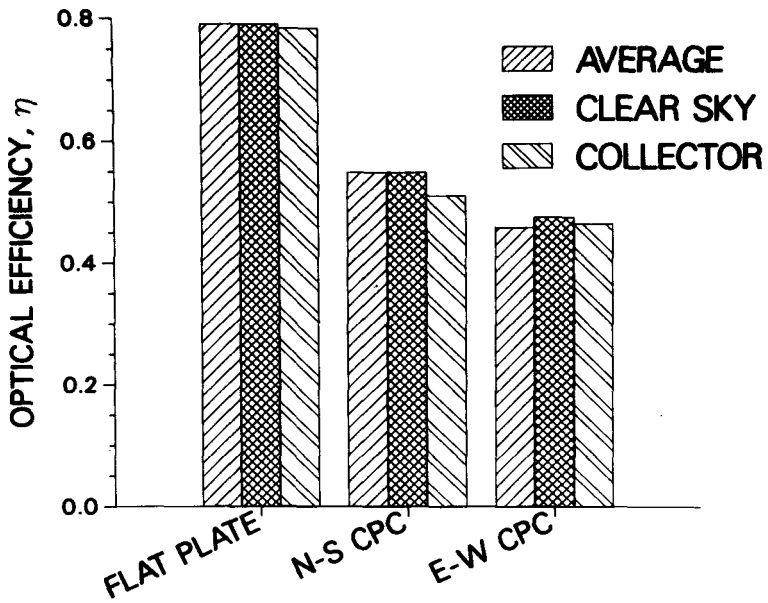

FIGURE 3.5 Run-Time Optical Efficiencies (Daily starting temperature of storage is 30°C.)

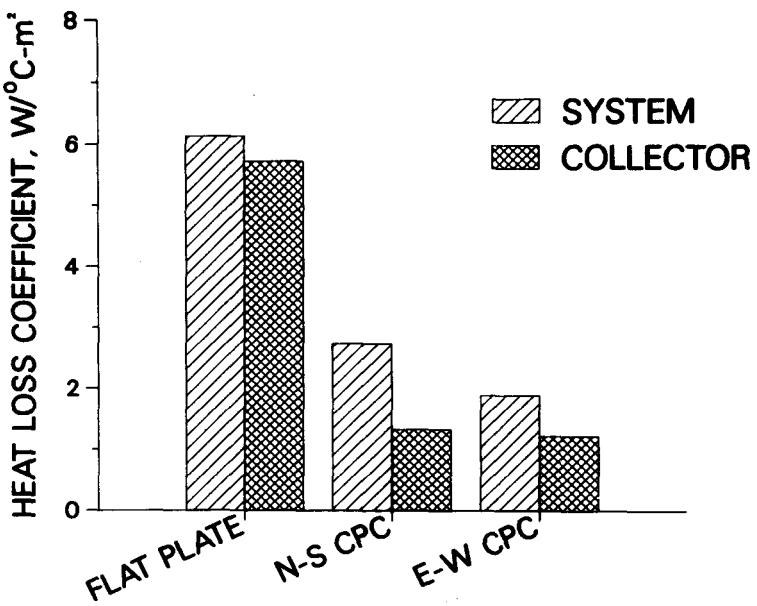

FIGURE 3.6 Run-Time Heat-Loss Coefficients (Daily starting temperature of storage is 30°C.)

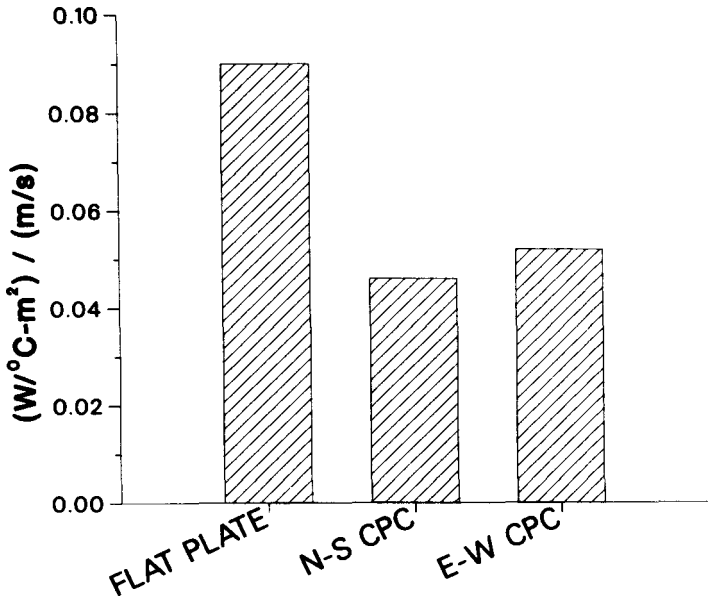

FIGURE 3.7 Run-Time Wind Effect (This is the increase in heat-loss coefficient caused by the wind, divided by the wind speed. Daily starting temperature of storage is 30°C.)

E-W CPC. This result would be expected, because the E-W CPC had an acceptance angle of only 72°; the N-S CPC and flat plate had acceptance angles of 110° and 180°, respectively. Thus, the E-W CPC excluded a greater fraction of the insolation on cloudy or hazy days. The effects of diffuse insolation are shown by plotting two different run-time optical efficiencies. The bars in Figure 3.5 labeled "average" indicate average values of η and were obtained by eliminating the diffuse fraction from the regression. The bars labeled "clear sky" indicate η', a measure of the optical efficiency that would result if the skys were clear every day. The value of a_D obtained for the E-W CPC is 0.094, which indicates that the collector's optical efficiency on entirely diffuse days was 0.094 less than the clear-sky value.

Figure 3.5 also presents optical-efficiency parameters, η, for the collectors at normal incidence. These parameters were obtained from independent analyses of the collectors alone. The systems' run-time optical efficiencies were almost identical to the collectors' optical efficiencies. The differences between the CPC systems' clear-sky values and the CPC collectors' normal-incidence values probably resulted from the increase in CPC optical efficiency at off-normal incidence angles. The beneficial effects of this increase can appear in system tests but not in normal-incidence collector tests.

In Figure 3.6, each system's run-time thermal loss coefficient, U, is compared with the collector's overall loss coefficient, U_L, which was obtained from an independent analysis of each collector. The systems' run-time thermal-loss coefficients were higher than the collectors' loss coefficients, because piping and storage losses were reflected in

the systems' coefficients. The differences between collector and system coefficients were greater for the CPCs than for the flat plate, because CPC thermal losses comprised a smaller fraction of total system losses.

Figure 3.7 displays the values of the wind effect, a_W, obtained from the regressions using run-time data. Comparisons of wind effects clearly show the reduced significance of convective heat transfer that resulted when evacuated tubes were used as solar absorbers.

Figures 3.8, 3.9, and 3.10 present results obtained by applying the model in Equations 1, 2, and 3 to entire-day data. These system parameters were obtained from data covering periods during the day when the collectors did not operate, as well as those periods when the collectors did operate. Thus, the parameters show the effects of differences in the run-time fractions among the three systems. These parameters were easier to obtain than the run-time parameters, because they were based on data on solar radiation, outdoor temperature, and wind speed averaged over the entire day rather than over the periods of collector operation. Instrumentation for system testing can be simplified if only these "daily" parameters are desired, because it is not necessary to record the frequency of collector operation.

Figure 3.8 shows that the effective daily optical efficiency of each system was less than the optical efficiency of the collector alone. The daily optical efficiency of the flat plate system was 27% less, and the daily optical efficiencies of the N-S and E-W CPCs were 13 and 16% less, respectively. The variations resulted from differences in the run-time fractions discussed in Section 3.2. The flat plate system was less able than the

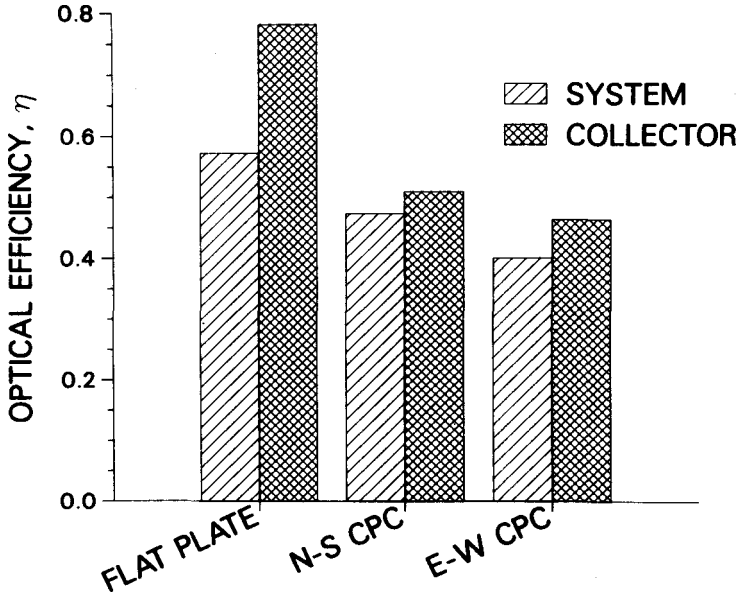

FIGURE 3.8 Daily System Optical Efficiencies Compared with Collector Optical Efficiencies (Daily starting temperature of storage is 30°C.)

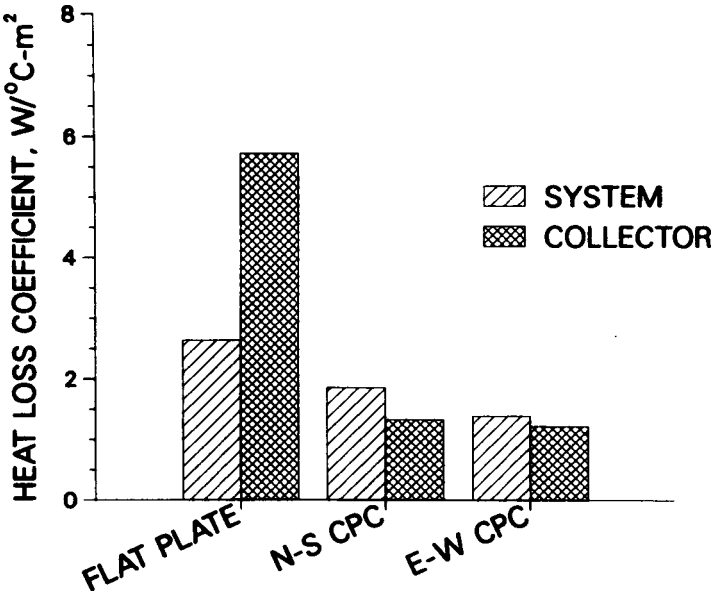

FIGURE 3.9 Daily Heat-Loss Coefficients (Daily starting temperature of storage is 30°C.)

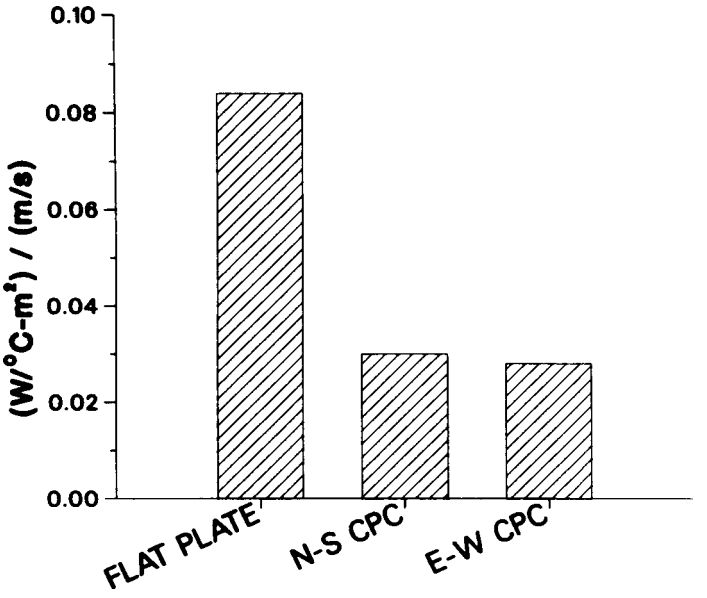

FIGURE 3.10 Daily Wind Effect (Daily starting temperature of storage is 30°C.)

CPC systems to realize its maximum optical efficiency (the collector's optical efficiency), because it collected energy less frequently.

Figure 3.9 compares each system's effective daily thermal-loss parameter with its collector's thermal-loss coefficient. The systems' effective daily thermal-loss rates were also reduced from their run-time values according to the run-time fractions (i.e., lower run-time fractions resulted in lower daily thermal losses). This reduction occurred because, when the systems were not operating, thermal energy was lost only from the storage tanks. A system's loss rate approaches its storage tank's loss rate as the run-time fraction approaches zero.

Figure 3.10 shows the wind effects (a_W) derived from entire-day data. The daily wind-effect parameters yield results similar to those obtained from the run-time wind parameters. The CPC collectors, with their evacuated absorber tubes, were affected by the wind much less than was the flate plate collector.

These system parameters represent a first step in the search for a set of parameters obtained from tests of complete systems rather than components. The general usefulness of these parameters remains to be determined. In the present context, they are useful for explaining differences in the performance of the three systems.

The system parameters described above, especially the entire-day parameters, may well vary significantly with climate. Thus, it may be necessary to obtain sets of these parameters for several different representative climates in order to fully characterize a system.

We have not yet explored ways of incorporating these parameters in a system-rating procedure. We do, however, discuss in Chapter 6 the need for a "universal" solar-heating-system simulation model that uses experimentally determined system parameters rather than component parameters. Parameters presented here, such as the run-time and daily system parameters, may possibly prove useful in developing such a model. This model, in turn, would be of use in developing a system-rating procedure.

3.4 SNOW AND ICE EFFECTS

In presenting the results of the side-by-side tests, we removed the effects of snow and ice covering the collectors by excluding data taken on days when the collectors were covered.

We can consider snow, ice, and frost coverage by comparing simulated and measured performance on days when all three collector arrays had significant coverage. Figure 3.11 shows the average daily energy gains of the three systems on 19 days in January and February of 1982. Table 3.2 presents a brief summary of conditions on each of the 19 days. Figures 3.12, 3.13, and 3.14 present measured and simulated results for the three collectors on each of the 19 days. These figures and Table 3.2 facilitate comparisons of actual and potential performance for each system for a variety of snow and ice conditions.

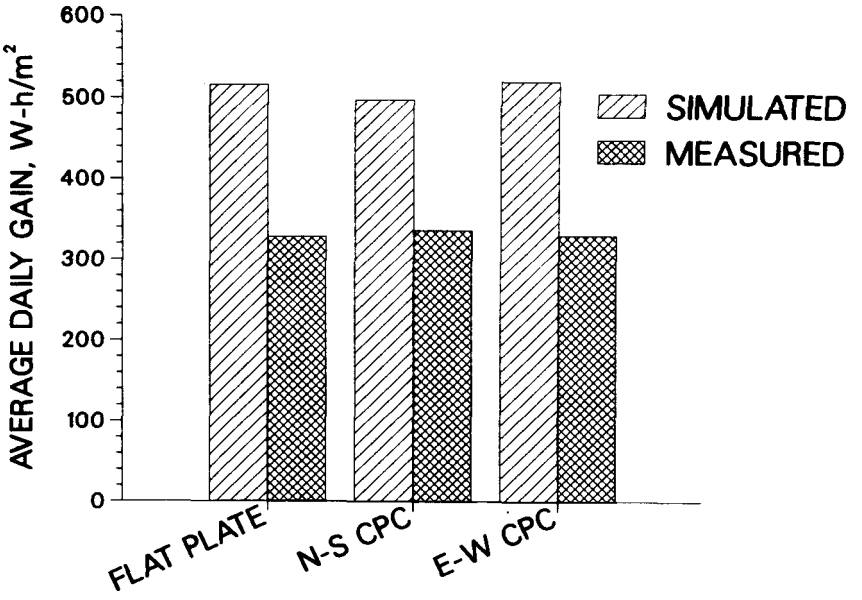

FIGURE 3.11 Average Daily Energy Gain during 19 Days with Snow, Ice, and Frost on Collectors (Daily starting temperature of storage is 30°C.)

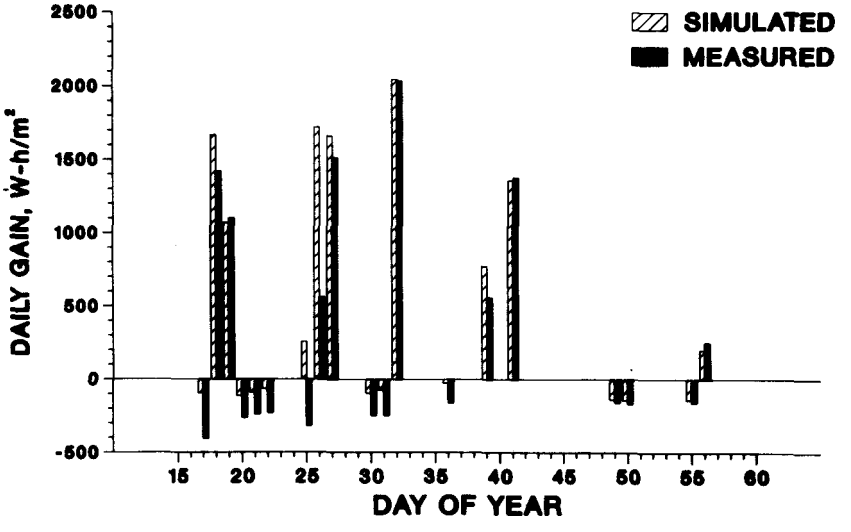

FIGURE 3.12 Energy Gain of Flat Plate System with Snow, Ice, and Frost (Daily starting temperature of storage is 30°C.)

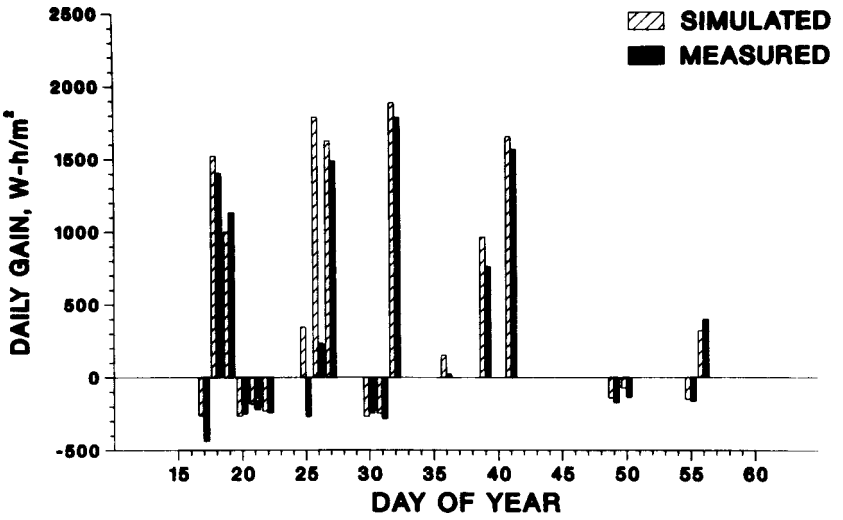

FIGURE 3.13 Energy Gain of N-S CPC System with Snow, Ice, and Frost (Daily starting temperature of storage is 30°C.)

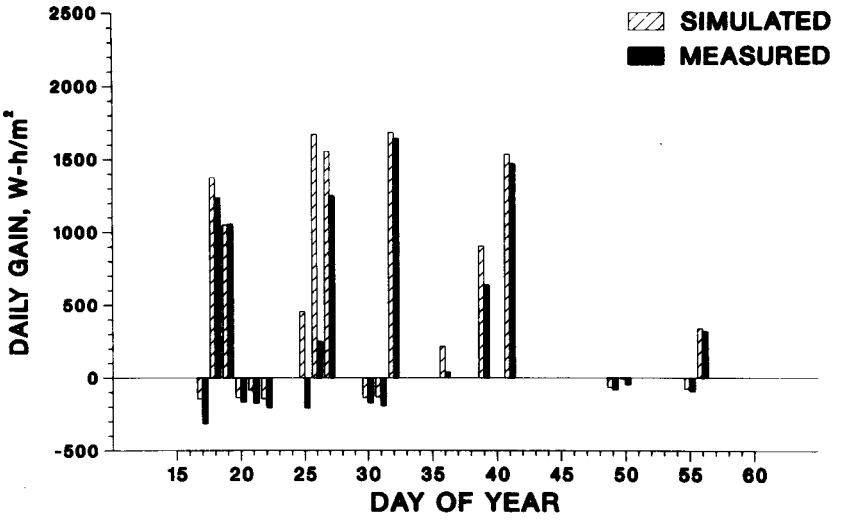

FIGURE 3.14 Energy Gain of E-W CPC System with Snow, Ice, and Frost (Daily starting temperature of storage is 30°C.)

TABLE 3.2 Days with Snow, Ice, or Frost

Day of Year	Description
17-22	Fresh snow fell on day 17 and remained on collectors during this period of very cold outdoor ambient temperatures until late on day 22, when the temperature rose to 4°C.
25-27	Fresh snow fell at midday on day 25 and remained until the afternoon of day 27.
30	Freezing rain coated all collectors with ice.
31	Fresh snow covered ice-coated collectors.
32	Snow was cleared by hand in early morning, but ice remained in troughs of N-S CPC.
36	Fresh snow covered all collectors until it was removed by hand at 13:00.
39	Frost on all collectors during much of the morning.
41	Frost on all collectors during much of the morning.
49	Snow fell all day.
50	Snow fell, but it melted due to rising temperatures.
55	Freezing rain coated all collectors with ice.
56	Fluffy, dry snow covered collectors and pyranometers.

This way of examining snow and ice effects is incomplete, because it does not account for differences in the rates at which snow and ice clear from the different types of collectors. Our data on this phenomenon are insufficient for two reasons. First, after most snowfalls snow and ice were cleared by hand from all three collector arrays within one or two days. Second, the tilt angle of the collector arrays (equal to latitude) was 10 to 15 degrees less than the angle normally used in most solar heating applications. The E-W CPC tilt angle had to be equal to ANL's latitude so that its optical performance would not deteriorate near the summer or winter solstices. However, N-S CPCs and flat plate collectors can be and often should be tilted at greater angles with respect to the horizontal. A greater tilt angle causes the snow to clear more easily and reduces the chance that ice will form. Further testing with the N-S CPC and with flat plate collectors at greater tilt angles and without snow removal is necessary to produce a more comprehensive assessment of snow and ice effects.

3.5 EFFECTS OF HIGHER-TEMPERATURE OPERATION

Tests were run with all three systems operating at higher temperatures during late June and early July of 1982. The temperature switch that controlled the nighttime energy-dumping heat exchanger was reset so that the initial morning storage temperature was 50°C rather than 30°C. Useful results were obtained for 27 days of operating with the N-S CPC and E-W CPC and for 10 days of operation with the flat plate system. Results from 17 days of flat plate operation at higher temperatures were omitted from the data, because on those days a temperature-switch malfunction caused the initial morning temperature to be much lower than 50°C.

Table 3.3 presents a summary of the results from higher-temperature operation. The flat plate system's performance decreased more than did the CPC system's performance as a result of higher-temperature operation. During the summer of 1981, at lower temperatures, the average daily gain of the N-S CPC was 6% less than that of the flat plate, and that of the E-W CPC was 28% less. During the higher-temperature tests in the summer of 1982, the gain of the N-S CPC was 4% less than that of the flat plate, and that of the E-W CPC was 9% less. The higher-temperature operation was conducted during the summer, which is the best season for flat plate collector performance. Table 3.3 also shows that the flat plate experienced the greatest drop in run-time efficiency (46%) and that the E-W CPC experienced the least drop. Thus, the relative performance of the E-W CPC improved the most at higher temperatures. This result confirms that the E-W CPC had the lowest thermal-loss coefficient, U_L, of the three collectors.

TABLE 3.3 Higher-Temperature Operation of Collector Systems (June and July, 1982)

	Flat Plate	N-S CPC	E-W CPC
Average Daily Gain ($W \cdot h \cdot m^{-2}$)	859	823	785
System Efficiency	0.22	0.21	0.20
Run-Time Fraction	0.36	0.58	0.66
Run-Time Efficiency	0.29	0.26	0.23
Decrease in Run-Time Efficiency from Average 1981 Summer Performance (%)	46	38	34

4 SELECTION AND VALIDATION OF ANALYTICAL SIMULATION MODEL

4.1 EXTENDING TEST RESULTS BY SIMULATION MODELING

The value of long-term side-by-side tests can be significantly enhanced by computer simulation. A computer simulation model is used to examine the effects of changes in test conditions and equipment designs in a short time and at low cost. To study such changes experimentally would require a great deal of time and expense.

Measured performance data are necessary to calibrate and validate a simulation model. Long-term measured performance results are very useful for validation, because comparisons of measured and simulated performance can be made over the entire range of operating conditions. However, short-term tests that subject the system to a range of different operating conditions might be adequate to validate a model. This issue is addressed in Chapter 6.

4.2 REASONS FOR SELECTING ANSIM

The solar-heating-simulation model ANSIM (Analytical Simulation) was selected for validation and for simulated side-by-side comparisons.[8] This model was selected for two reasons. First, ANSIM requires much less computing time than other models, such as TRNSYS[10] (see Section 4.3). The reduction in computing time is accomplished by using analytical solutions to the storage energy balance and by tailoring the computer code to the common configuration of components, such as a collector array, a storage tank, and a load loop. This configuration can also be modeled using simplified design methods such as f-Chart.[3] However, f-Chart is a regression equation and is valid only for a limited range of operating conditions and component designs; it is not appropriately used to simulate side-by-side comparisons of systems distinguished by subtle differences in collector optics and system control strategies.

The second reason for using ANSIM involves its potential for implementation on a microcomputer. The ANSIM model was developed on a minicomputer (Digital Equipment Corporation, PDP-11) possessing a memory capacity equivalent to the capacities of microcomputers being used with increasing frequency in the solar-energy industry. In Chapter 6, we propose future research on methods of combining short-term system tests with a simulation model for the evaluation and rating of solar-heating systems. The usefulness of such methods would be enhanced if microcomputers could be used for system simulation. It seems likely that ANSIM could provide a starting point for the development of a simulated system testing and rating method.

The ANSIM model can be operated either as an hourly model or as a daily model. When hourly time steps are used, it is assumed that the average values for the driving forces (such as solar radiation and outdoor temperature) for each hour adequately represent the instantaneous values at the midpoint of the hour. Instantaneous values at other times are expressed as linear functions defined by interpolation between adjacent hourly values. For this reason, the hourly ANSIM model is also referred to as the linear ANSIM model (L-ANSIM).

When daily time steps are used in the daily ANSIM model (D-ANSIM), each day is divided into two time steps. The first step begins at sunrise and ends at sunset; the second step begins at sunset and ends at sunrise of the next day. Parabolas are used to describe variations in the driving forces during each daily step. The three coefficients of each parabola are obtained from a least-squares fit to hourly data. Smoothing of the data in this fashion removes the random fluctuations in the driving forces (especially insolation) while retaining the important trends in the data for each day. Furthermore, the effects of incidence-angle modifiers and variations in the relative amounts of beam, sky, and ground radiation are taken into account on an hourly basis, and a daily parabola is fitted to hourly values of absorbed energy. Thus, the smoothed driving forces are those that affect the thermal, rather than the optical, response of the system. The thermal response is somewhat insensitive to random fluctuations in the driving forces because of the amount of thermal energy stored in the mass of the system.

The simulated side-by-side comparisons presented in Chapter 5 were produced using the L-ANSIM model. We show in Section 4.3 that the D-ANSIM model produces results that are very closely comparable with the results of the L-ANSIM and TRNSYS models. Therefore, the D-ANSIM model, with its reduced data-storage and computation requirements, should be considered for inclusion in a microcomputer-based system testing and rating procedure.

4.3 COMPARISON OF ANSIM MODELS WITH TRNSYS MODEL

In this section, we compare the results from the L-ANSIM model, D-ANSIM model, and the TRNSYS Version 11.1 model. A typical residential solar space-heating system with 50 m^2 of flat plate liquid-type collectors and 4 m^3 of water-based thermal storage was simulated using weather data from Madison, Wisconsin, for the year 1954. The system was similar to the "Detailed Liquid Solar Heating System" used in Example No. 11 of the manual for TRNSYS Version 11.1, except that the domestic water-heating load was not included. These weather records were used by the International Energy Agency[11] in comparisons of several different solar-heating simulation models. All three models were run on a single computer, a VAX-11/780, using the virtual-memory operating system (VMS).

For all runs, the models were programmed to produce only monthly and annual performance summaries. Thus, similar numbers of output operations were required for each model. However, the number of input operations was not the same. The L-ANSIM model and the TRNSYS model read each hour's data on driving forces from a disk and processed the radiation data, accounting for collector tilt, incidence angle, and optical efficiency each simulated hour. On the other hand, the D-ANSIM model loaded the entire year of preprocessed data (coefficients of parabolas for each day and night period) into the main memory at the beginning of program execution.

The following component models were used in the TRNSYS runs ("Type" numbers identify the specific TRNSYS program modules used): Type 16, Radiation Processor; Type 1 (Mode 4) Solar Collector; Type 2, Controller; and Type 4, Storage Tank (used with one segment, not stratified).

Table 4.1 presents the CPU times required by each model to produce the predicted performance results. Table 4.2 presents the predicted performances for four months during the heating season and for the entire year. Comparisons of the TRNSYS-model and L-ANSIM-model predictions presented in Table 4.2 reveal that the two models produced almost identical results. However, use of L-ANSIM required substantially less computer time.

There are two primary reasons for the D-ANSIM model requiring less computer time. First, TRNSYS is designed for great flexibility in the types of system configurations it can examine; this feature requires a scheme for connecting many different types of components and results in slower computation speeds, even for simple systems. Second, the driving period used in TRNSYS must be kept short, because a change in the TRNSYS operating mode can be made only at the beginning of a driving period. (The driving forces in TRNSYS are held constant at their average values during the driving period.) In order to obtain the close correspondence between the results from L-ANSIM and TRNSYS, TRNSYS was run with a driving period (time step) of 15 min.

The TRNSYS model can be configured to run efficiently (although slightly less accurately) with hourly time steps by using a combined collector-storage module (Type 21). Running TRNSYS in this configuration on the sample problem required 149 s of CPU time. The predicted annual solar fraction was 0.726, slightly higher than the fraction predicted by TRNSYS using 15-min time steps.

TABLE 4.1 CPU Run Times Required by Each Model[a] (s)

L-ANSIM	D-ANSIM	TRNSYS
63	16[b]	347[c]

[a]All models were run on a VAX-11/780 computer using the VMS.

[b]In another run of daily ANSIM, 25 different designs -- each involving a different combination of collector area and storage volume -- were examined. The total CPU time was 3 min 48 s (9 s per design).

[c]A slightly less accurate configuration of TRNSYS using a combined collector-storage module and one-hour time steps requires 149 s of CPU time.

TABLE 4.2 Comparison of Annual Performance Predicted by Each Computer Model

Period	Computer Model	Collector Efficiency	Average Storage Temp (°C)	Energy from Storage to Load (10^6 kJ)	Solar Fraction	Collector On-Time (h)	Auxiliary On-Time[a] (h)
January	L-ANSIM	0.370	29.54	6.328	0.488	154.7	551.4
	D-ANSIM	0.364	29.52	6.340	0.489	174.6	546.1
	TRNSYS	0.367	29.60	6.355	0.491	-	-
March	L-ANSIM	0.314	59.39	7.550	0.946	174.3	62.4
	D-ANSIM	0.307	58.59	7.540	0.940	196.0	68.2
	TRNSYS	0.313	59.50	7.552	0.946	-	-
September	L-ANSIM	0.229	92.12	1.168	1.0	151.1	0.0
	D-ANSIM	0.214	91.97	1.231	1.0	164.3	0.0
	TRNSYS	0.228	92.21	1.168	1.0	-	-
November	L-ANSIM	0.333	48.33	4.902	0.704	129.2	212.9
	D-ANSIM	0.327	47.90	4.851	0.695	145.5	214.7
	TRNSYS	0.327	48.47	4.919	0.706	-	-
All Year	L-ANSIM	0.261	68.58	42.00	0.708	1870	1639
	D-ANSIM	0.247	68.08	42.28	0.708	2099	1638
	TRNSYS	0.260	68.65	42.10	0.709	-	-

[a]"Auxiliary On-Time" is the total time during which the solar heating system is incapable of supplying the entire heating load. A furnace actually operates by cycling on and off during each period of auxiliary heating, so furnace operating time (not shown) is less than "Auxiliary On-Time."

Comparison of the D-ANSIM and L-ANSIM predictions presented in Table 4.2 shows that very little accuracy was lost by using smoothed data and daily driving periods. In fact, for this example, the annual solar fractions were identical. The largest error occurred in November, when the use of D-ANSIM caused the solar fraction to be underestimated by 1.3%.

The run of D-ANSIM that produced the results in Table 4.2 required 16 s of CPU time. However, a run that examines a single system design does not fully exploit the advantages of a daily model. Another run of D-ANSIM examined 25 different combinations of collector area and storage volume and produced 25 annual performance summaries as output. This run required 3 min 48 s of CPU time, or only 9 s per design. The data from these runs are not presented.

The increase in speed of analysis from 0.95 designs per CPU minute (63 s per design) with L-ANSIM to 6.7 designs per CPU minute (9 s per design) with D-ANSIM represents a sevenfold increase in computing speed. This improvement makes it possible to introduce computer simulation, with its flexibility regarding allowable ranges of component parameters and design variables, into a microcomputer-based design, evaluation, and rating procedure for solar heating systems.

4.4 VALIDATION OF ANSIM FOR EXPERIMENTAL SYSTEMS

Runs of the L-ANSIM model were made using solar-radiation and outdoor-temperature data collected at the test site and averaged over one-hour periods. Separate measurements of beam, sky, and ground-reflected radiation on the tilted collector array were not available, but estimates of these components were necessary to determine the energy absorbed by an absorber. We applied the correlation of Boes et al.[9] to measurements of global radiation on a horizontal surface to separate the beam and sky components. Radiation reflected from the ground was assumed to be diffuse and was calculated using global horizontal radiation and an estimate of ground reflectivity. Ground reflectivity was estimated to be 0.8, because the ground in front of the test site was covered by a white-gravel parking lot. The fractions of total radiation on the tilted array contributed by each component were determined trigonometrically. These fractions were applied to measurements of global radiation on the tilted array to obtain estimates of the three radiation components.

The optical efficiency of each CPC collector was calculated for each solar incidence angle by means of a ray-tracing program. Ray tracing was necessary because of the complex relationship between CPC optical efficiency and the angle of incidence of solar radiation. Actually, analysis of the CPC collectors required that the incidence angle be resolved into transverse and longitudinal components. The transverse component is the projection of the incidence angle onto a plane that contains the normal to the collector face and is perpendicular to the tubes (and troughs). The longitudinal component is the projection of the incidence angle onto a plane that contains the normal to the collector face and is parallel with the tubes (and troughs). The variation of CPC optical efficiency with the longitudinal component was very smooth and not unlike the variation of a flat plate collector's optical efficiency with incidence angle. However, the variation of CPC optical efficiency with the transverse component was very complex.

Figure 4.1 shows the variation in optical efficiency with the transverse component of the incidence angle for an advanced experimental CPC collector that was constructed and tested at ANL for the production of steam. The absorptance of the absorber tubes was 0.95, and the reflectance of the concentrators was 0.95. Also shown in Figure 4.1 is the much smoother variation in optical efficiency with incidence angle for a flat plate collector.

When the CPC collector systems were modeled, ray tracing was performed for each hour of simulated performance. The N-S CPC required tracing of 100 rays for each incidence angle; the E-W CPC, with its higher concentration, required 150 rays for each incidence angle. An alternative to ray-tracing for every simulated hour that would significantly reduce computing time is the computation of biaxial incidence-angle modifiers for a large number of different values of the transverse and longitudinal components of the incidence angle. The incidence-angle modifier for a specific hour could then be calculated by interpolation. This procedure should be incorporated.

A theoretical model of flat plate collector optics by Duffie and Beckman[12] was used to determine incidence-angle modifiers for the flat plate system. With all three systems, separate optical efficiencies were calculated for each of the three components of solar radiation (beam, sky, and ground).

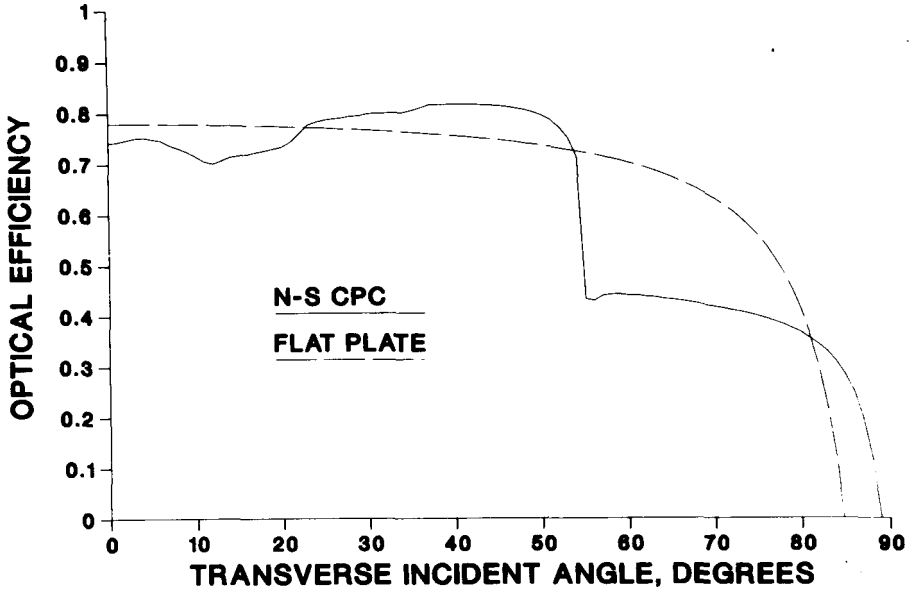

FIGURE 4.1 Optical Efficiency vs. Transverse Incidence Angle for an Advanced N-S CPC and a Flat Plate Collector

In general, the experimentally determined collector parameters $F_R\eta_o$ and F_RU_L supplied by the collector manufacturers were used in the simulations.* The single exception to using the collector parameters supplied by the manufacturers involved the optical efficiency of the E-W CPC. The parameter $F_R\eta_o$ supplied by the collector manufacturer for the E-W CPC was slightly higher than that predicted by the ray-tracing program (which assumes a perfectly constructed collector), and using the collector parameters supplied by the manufacturer yielded simulated performance results that were consistently slightly higher than measured performance results. When optical efficiencies predicted by the ray-tracing program were used in the simulation model, excellent correspondence of measured and simulated performance was obtained.

The storage-tank loss coefficients supplied by the manufacturer turned out to be too low, so these coefficients were determined by comparing simulated and actual storage losses for days on which the collectors did not operate at all. The piping between the collector arrays and the storage tanks was well insulated and short (8 m), so thermal losses from the piping were not included explicitly in the simulation.

Table 4.3 gives the values of the parameters used in the simulation models to represent the three systems. These parameters, with one exception (described below), were held constant throughout the entire year of simulated time.

TABLE 4.3 Component Parameters for the Three Collector Systems

Component/Property	Flat Plate	N-S CPC	E-W CPC
Collector			
Area (m^2)	4.46	3.90	5.20
$F_R\eta_o$	0.78	0.51	0.48
F_RU_L ($W\cdot°C\cdot m^{-2}$)			
Summer	5.73	1.33	1.22
Rest of year	5.73	2.00	1.22
Higher temperature	5.73	2.39	2.20
Storage			
Volume (m^3)	0.348	0.348	0.348
Thermal loss ($W\cdot°C\cdot m^{-2}$)	1.03	1.03	0.68

*F_R is the solar collector heat-removal factor; η_o is the optical efficiency at normal incidence; and U_L is the solar collector heat-transfer loss coefficient.

The thermal-loss coefficient (U_L) of the N-S CPC collector was found to vary significantly between summer and winter. This effect was first noticed when comparisons of simulated and measured performances of the N-S CPC system yielded excellent agreement during the summer but poor agreement during the winter. The actual daily energy gain was less than that predicted by the model. (Similar comparisons for the flat plate and E-W CPC systems yielded excellent agreement in both summer and winter.) Damage to the N-S CPC system by ice and snow was at first hypothesized to account for the anomalous performance. The N-S CPC's reflector troughs were not protected by an extra sheet of glazing, whereas the E-W CPC's troughs were so protected. However, additional data showed that the thermal, rather than the optical, characteristics of the N-S CPC had changed during the winter. Close examination of performance data from May of 1981 and May of 1982 suggested that no permanent change in system performance parameters had occurred. Also, indoor heat-loss tests with the N-S CPC (conducted recently at ANL) have indicated that the thermal loss coefficient increases substantially as the temperature difference between the collector and the ambient laboratory air increases. The value of U_L has been found to increase by 100% as the temperature difference increases from 15 to 75°C. We conclude that the performance of the N-S CPC was degraded during the winter by an increase in the collector loss coefficient due to lower outdoor ambient temperatures.

Initial comparisons of measured and simulated performance of the N-S CPC system revealed a similar discrepancy in springtime values. However, the agreement between measured and simulated performance improved as the average daily outdoor temperature increased.

For the simulation of low-temperature operation (initial daily storage temperature at 30°C) in the validation comparisons of the next section and in the simulated comparisons of Chapter 5, the N-S CPC was modeled with $F_R U_L$ equal to 1.33 $W \cdot °C \cdot m^{-2}$ during summer and 2.00 $W \cdot °C \cdot m^{-2}$ during autumn, winter, and spring. The summer value was obtained from tests of the collector using the ASHRAE Standard 93-77 test procedure.[13] The value used for the rest of the year was obtained by increasing the test value of U_L by 50%. This increase was required to obtain agreement between measured and simulated results, and it was supported by our indoor heat-loss tests. The flat plate and E-W CPC systems were modeled with a constant U_L throughout the year for low-temperature operation.

Twenty-seven days of system operation at higher temperatures (initial daily temperature at 50°C) during June and July of 1982 provided data for a higher-temperature validation of the simulation model. During this period, the collector heat-loss coefficients, U_L, for both the N-S CPC system and the E-W CPC system had to be increased to obtain agreement between measured and simulated results. The loss coefficients for both collectors were increased by 80%. The simulated higher-temperature comparisons used the higher U_L values for both systems over the entire year. It was not necessary to increase the flat plate collector's U_L to obtain agreement during high-temperature operation. Results presented in Chapter 3 (showing a relatively low run-time fraction for the flat plate system) indicate that the flat plate collector does not operate at all under the extreme conditions that produce higher loss coefficients in the CPC collectors.

4.5 COMPARISON OF MEASURED AND SIMULATED PERFORMANCE

Figures 4.2-4.4 present comparisons of measured and simulated performance of the N-S CPC system, the E-W CPC system, and the flat plate system for 16 days during July 1981. Figures 4.5-4.7 present comparisons for 16 days in February 1982. The agreement is excellent for all three systems during both periods of operation. Figures 4.8-4.10 present comparisons for the period in June and July of 1982, when the initial morning storage temperatures were set at 50°C. Some days are missing from the flat plate system comparisons because of equipment failures. The agreement between measured and simulated performance is good for all three systems.

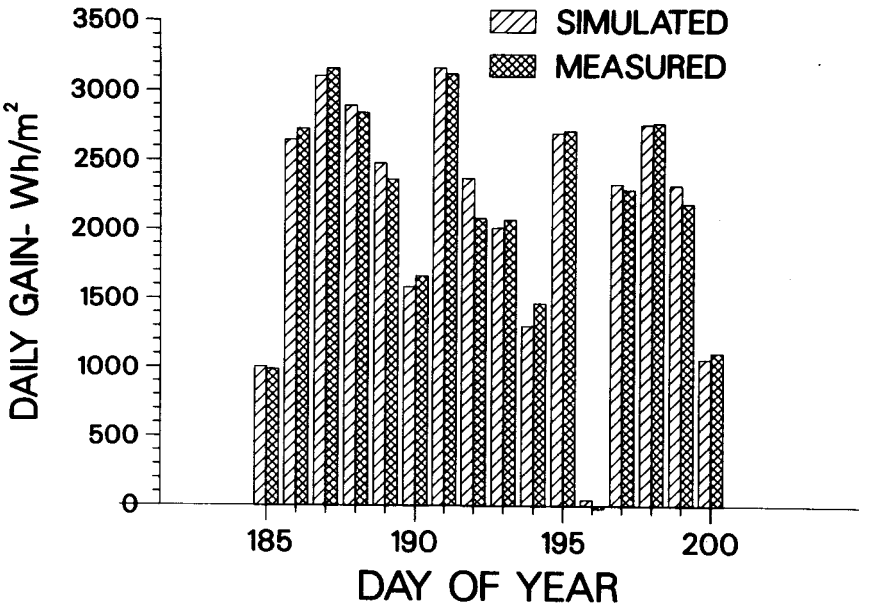

FIGURE 4.2 Low-Temperature Performance of Flat Plate System during Summer (July 4-19, 1981: Days 185-200. Daily starting temperature of storage is 30°C.)

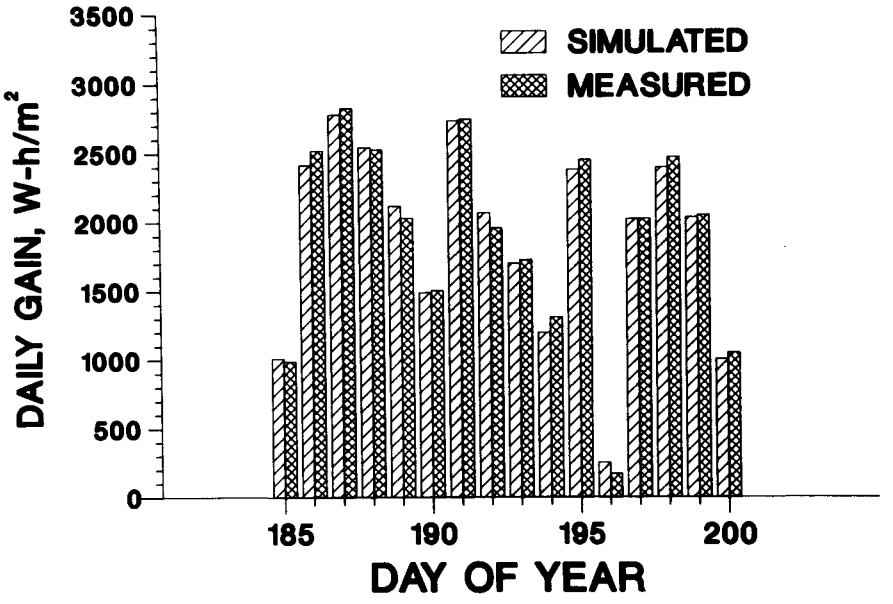

FIGURE 4.3 Low-Temperature Performance of N-S CPC System during Summer (July 4-19, 1981: Days 185-200. Daily starting temperature of storage is 30°C.)

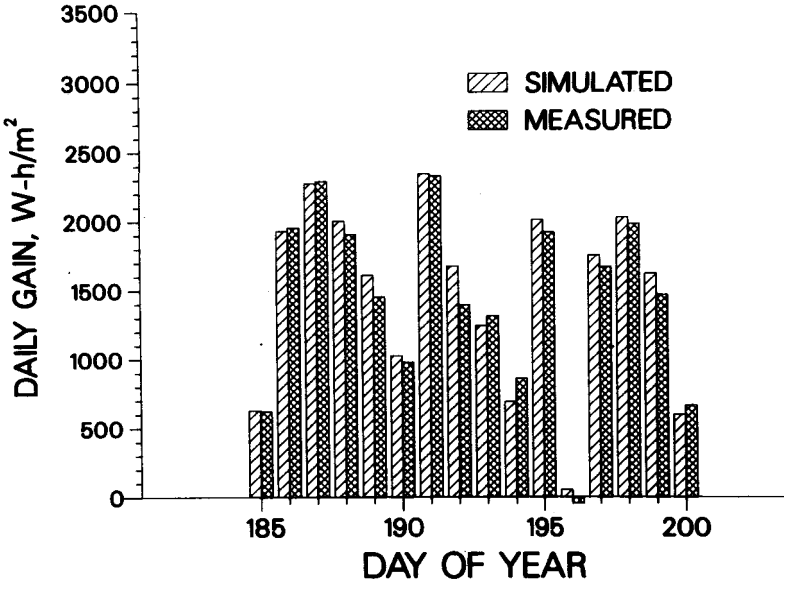

FIGURE 4.4 Low-Temperature Performance of E-W CPC System during Summer (July 4-19, 1981: Days 185-200. Daily starting temperature of storage is 30°C.)

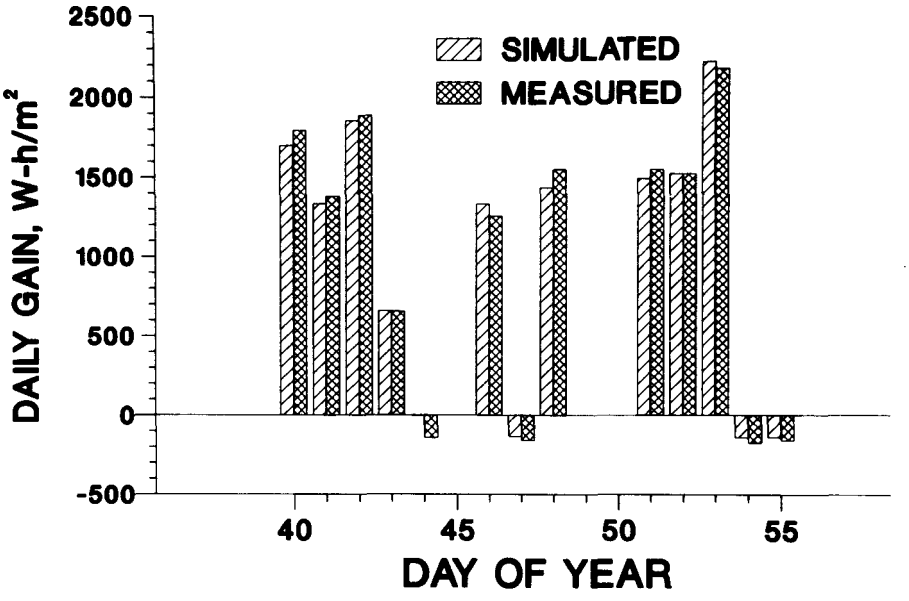

FIGURE 4.5 Low-Temperature Performance of Flat Plate System during Winter (February 9-24, 1981: Days 40-55. Daily starting temperature of storage is 30°C.)

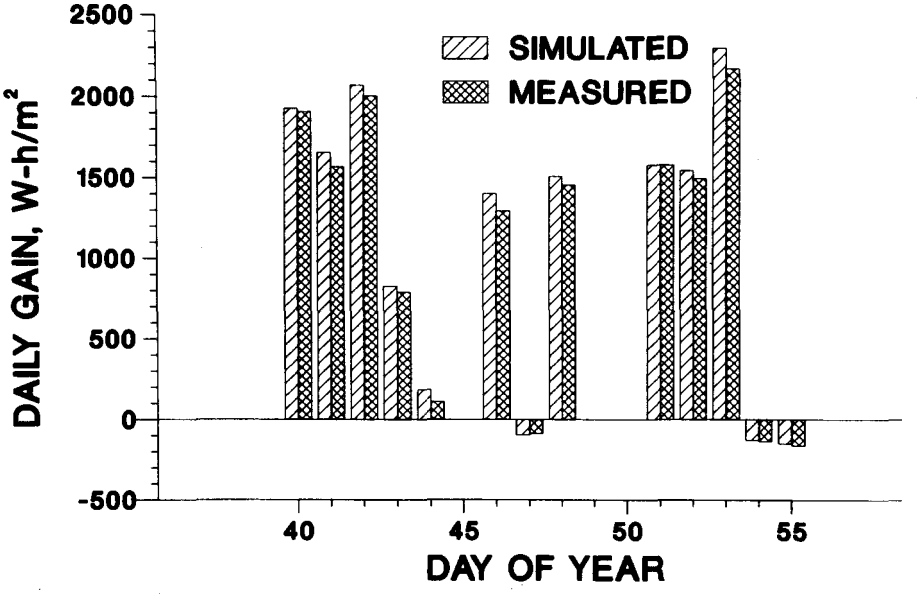

FIGURE 4.6 Low-Temperature Performance of N-S CPC System during Winter (February 9-24, 1981: Days 40-55. Daily starting temperature of storage is 30°C.)

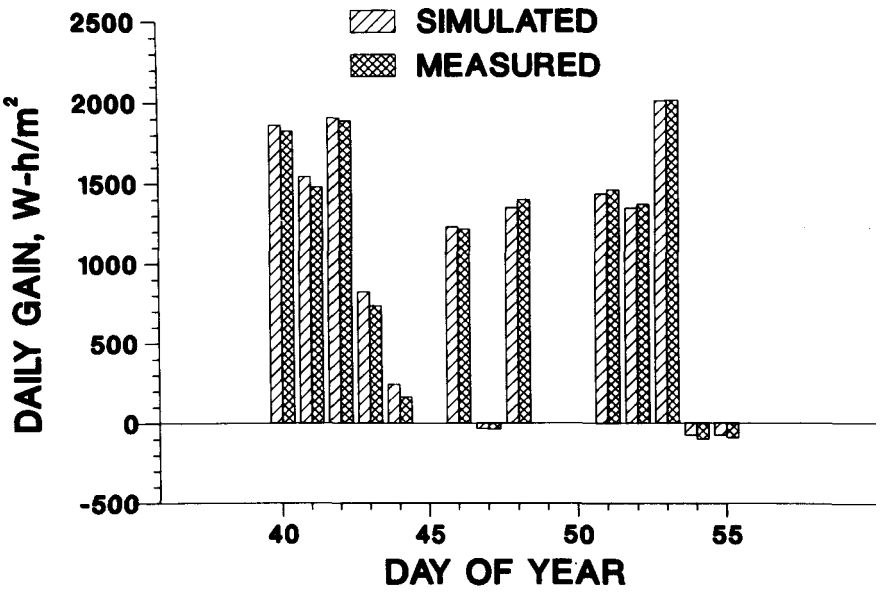

FIGURE 4.7 Low-Temperature Performance of E-W CPC System during Winter (February 9-24, 1981: Days 40-55. Daily starting temperature of storage is 30°C.)

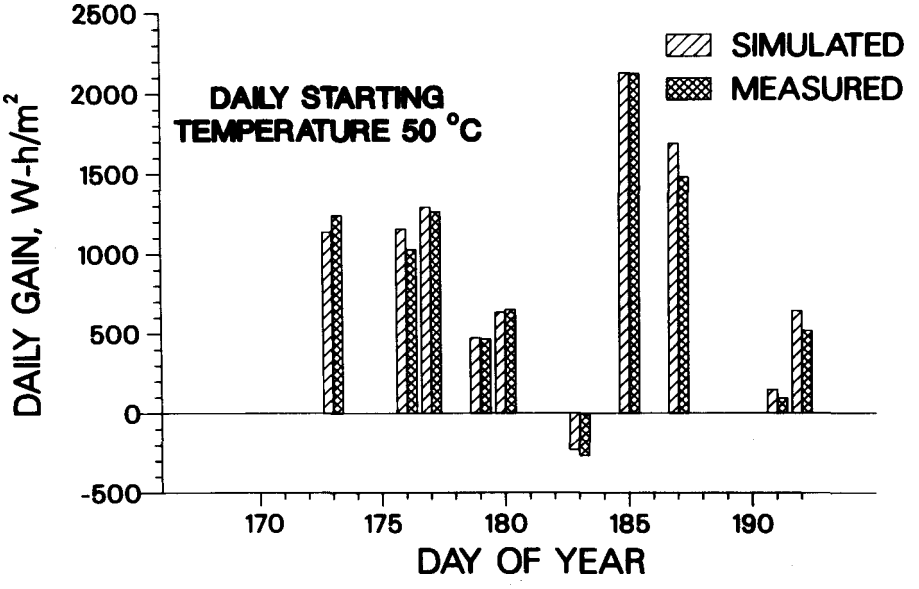

FIGURE 4.8 Higher-Temperature Performance of Flat Plate System during Summer (June 19-July 11, 1982: Days 170-192)

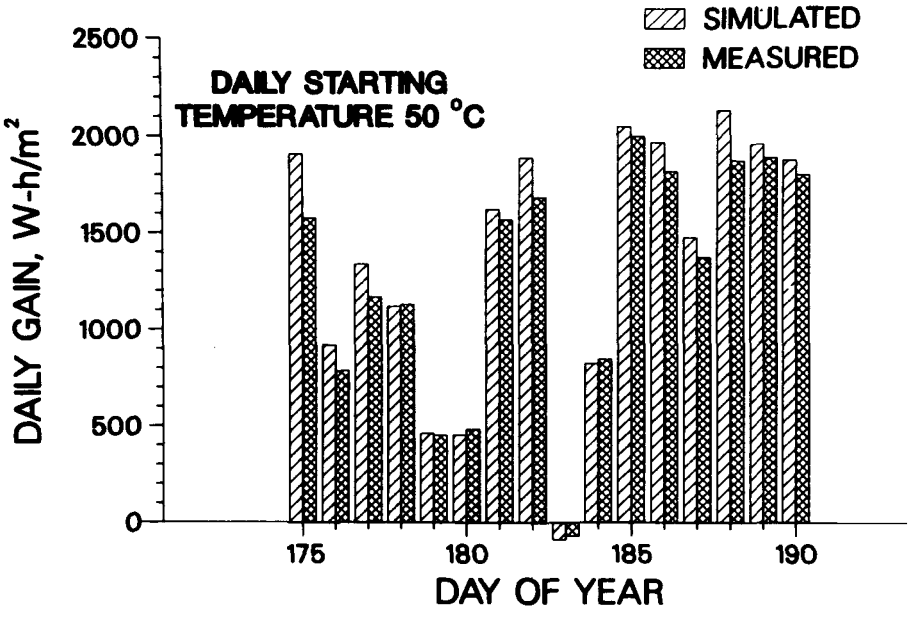

FIGURE 4.9 Higher-Temperature Performance of N-S CPC System during Summer (June 19-July 11, 1982: Days 170-192)

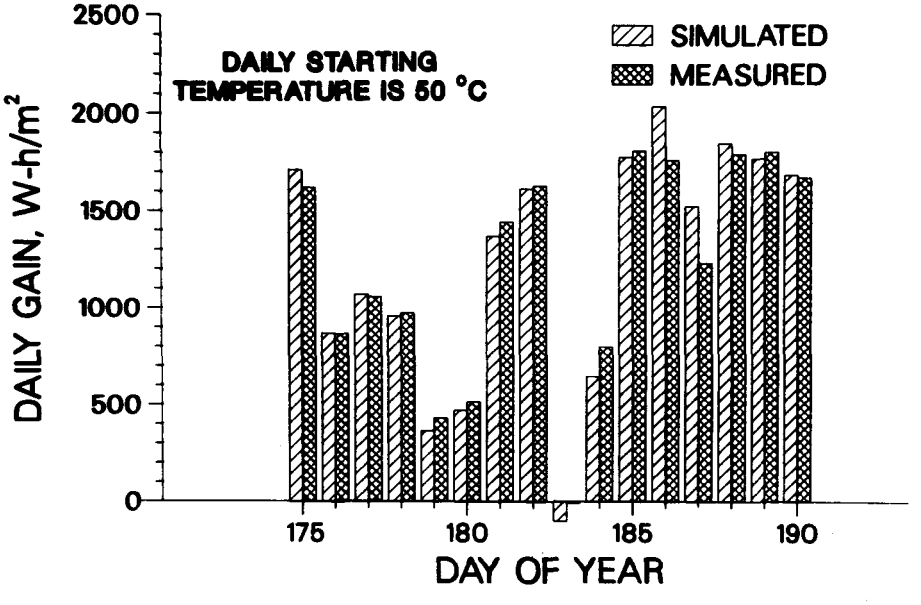

FIGURE 4.10 Higher-Temperature Performance of E-W CPC System during Summer (June 19-July 11, 1982: Days 170-192)

5 SIMULATED SIDE-BY-SIDE TESTS

The simulated side-by-side tests presented in this chapter are extensions of the actual side-by-side tests. A validated hourly ANSIM model for each system was used to examine system performance under conditions that differ from the actual conditions of the 1981-82 tests. The validated models were used to perform simulated side-by-side tests for six different cases.

5.1 COMPARISONS OF TESTED COLLECTORS USING 30°C DAILY STARTING STORAGE TEMPERATURE

The first three simulated side-by-side tests were simple extensions of comparisons of the three collectors tested at ANL. The daily starting storage temperature in these simulations was 30°C in all three systems, as it was in the actual tests. Changes were made only in the weather data in Sections 5.1.1 and 5.1.2. Comparisons in Section 5.1.3 showed the effects of simple modifications (orientation and cover-glass removal) on the performance of the E-W CPC collector system.

5.1.1 Three-Year Comparisons

The data required to examine the performance of the three systems at ANL are available for three complete years -- 1976, 1977, and 1980. We ran the ANSIM model for each system for these years to determine whether the relative performance results obtained from the 1981-82 tests were representative of long-term performance with the 30°C daily starting temperature. Figures 5.1, 5.2, and 5.3 present simulated bimonthly performance results with the 30°C starting temperature for the three years. Table 5.1 presents comparisons of total annual useful energy delivered by the collectors for each of the three years.

The rankings of the systems according to the annual totals of delivered energy were the same for all three years and agreed with the results presented in Chapter 3 for measured performance during 1981-82. However, the relative rankings of the flat plate and the E-W CPC systems for the months of January and February did vary with year. The N-S CPC outperformed both of the other collectors in January and February in all years, but the E-W CPC outperformed the flat plate in January and February in only two out of the three years.

5.1.2 Comparisons in Different Climates

We also compared the performance of the three different systems in two other cities. The two cities' climates differ from each other and from that of ANL. Medford, Oregon, represents a coastal climate. The winters are milder in Medford than at ANL; the outdoor ambient temperature does not reach the low extremes experienced at ANL. However, Medford experiences more cloudy weather. Albuquerque, New Mexico, represents a warm, arid, sunny climate. The weather data for Medford and Albuquerque were obtained from the SOLMET data base of the U.S. Department of Commerce.[14]

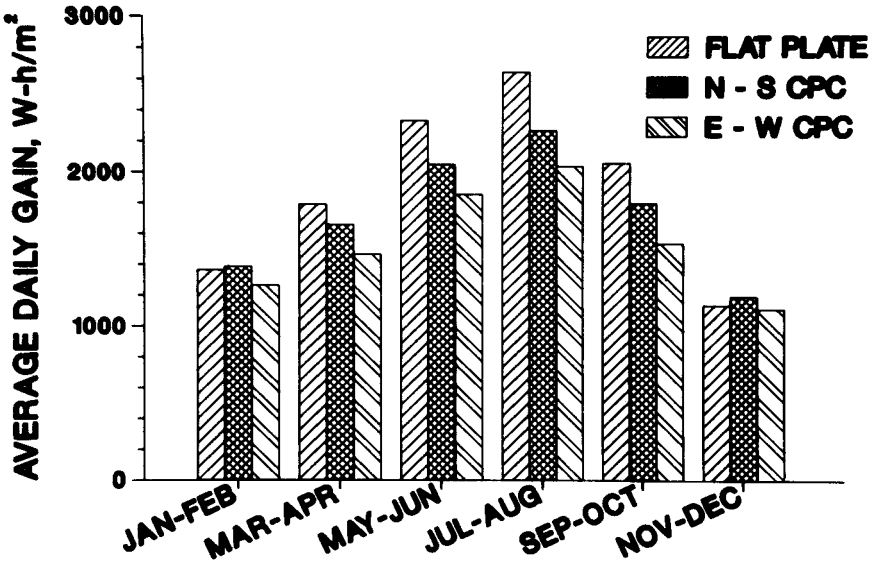

FIGURE 5.1 Simulated Collector Performance at ANL, Based on 1976 Weather Data (Daily starting temperature of storage is 30°C.)

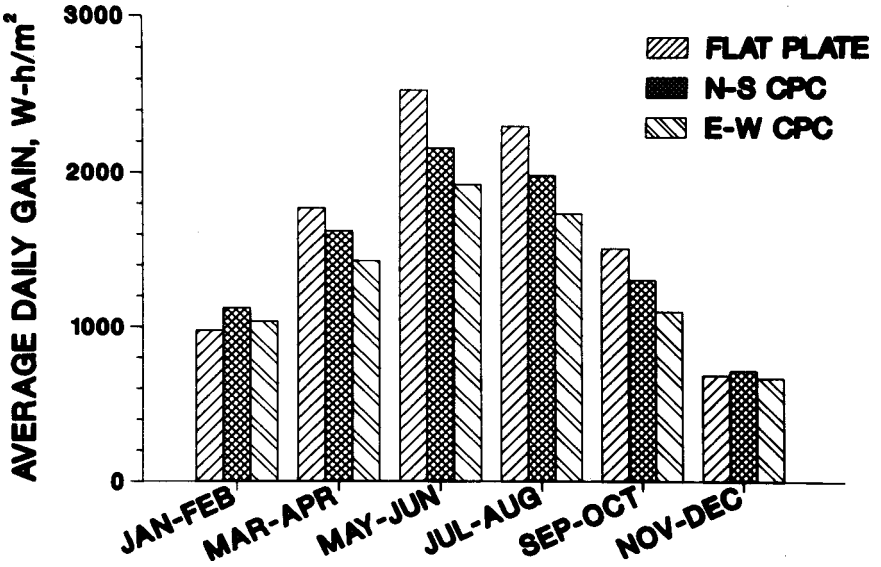

FIGURE 5.2 Simulated Collector Performance at ANL, Based on 1977 Weather Data (Daily starting temperature of storage is 30°C.)

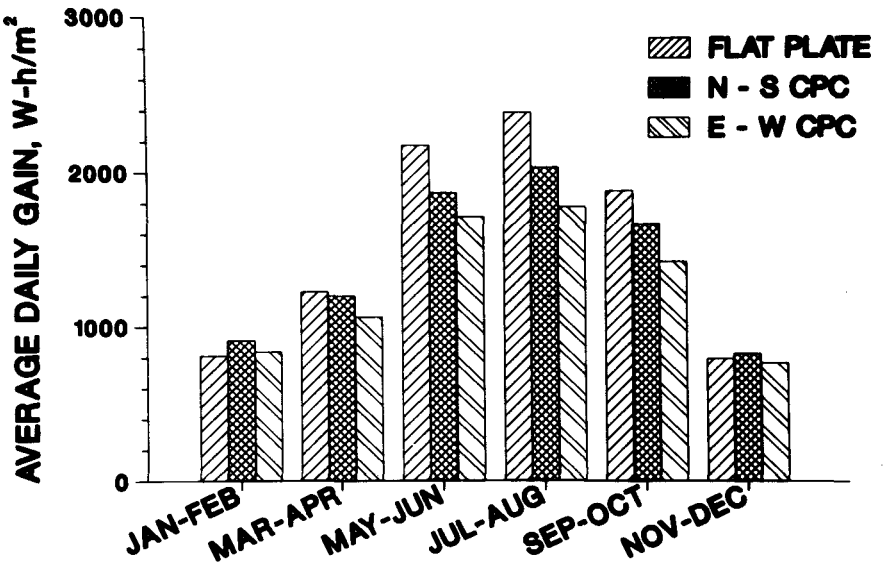

FIGURE 5.3 Simulated Collector Performance at ANL, Based on 1980 Weather Data (Daily starting temperature of storage is 30°C.)

TABLE 5.1 Comparisons of Simulated Energy Delivered Annually by the Systems for Three Different Years[a] ($kW \cdot h \cdot m^{-2} \cdot year^{-1}$)

System	1976	1977	1980
Flat Plate	691	597	569
N-S CPC	633	544	521
E-W CPC	568	482	464

[a]1980 ANL weather data; daily starting temperature of storage is 30°C.

Table 5.2 presents comparisons of annual totals of energy delivered by the collectors. Figures 5.4 and 5.5 present comparisons of average daily gains for different times during the year in Medford and Albuquerque, respectively (daily starting temperature of storage was still 30°C). In Albuquerque, the flat plate system was superior to the CPC systems during every month. However, relative rankings for the different seasons were very similar at ANL (Figure 5.3) and in Medford (Figure 5.4). We conclude that during the winter the relative performance of CPC systems improved at ANL because of the cold weather and in Medford because of the cloudy weather.

TABLE 5.2 Comparisons of Energy Delivered Annually in Three Different Climates ($kW \cdot h \cdot m^{-2} \cdot year^{-1}$)[a]

System	Medford, Oregon (1952)	Albuquerque, New Mexico (1953)	Chicago (1976)
Flat Plate	680	1102	691
N-S CPC	627	952	633
E-W CPC	561	816	568

[a]Daily starting temperature of storage is 30°C.

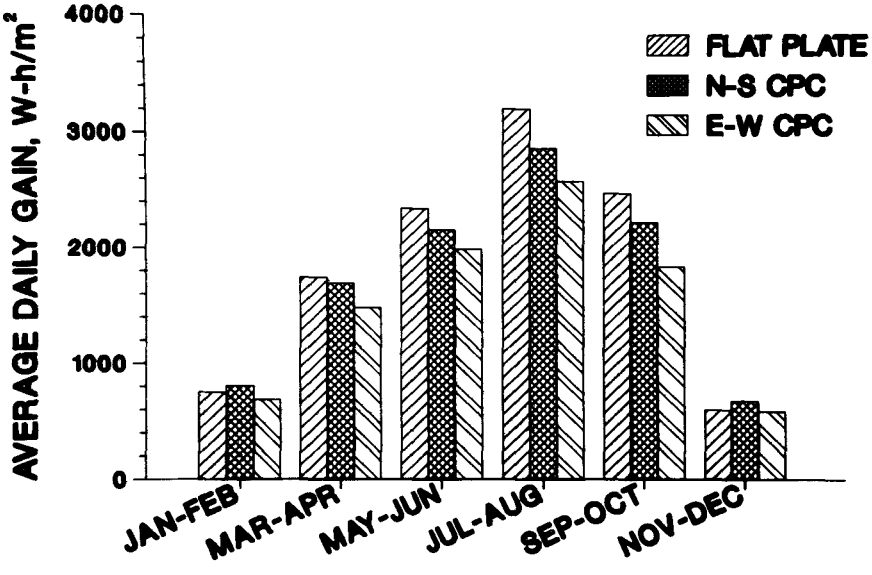

FIGURE 5.4 Simulated Collector Performance at Medford, Oregon, Based on 1952 Weather Data (Daily starting temperature of storage is 30°C.)

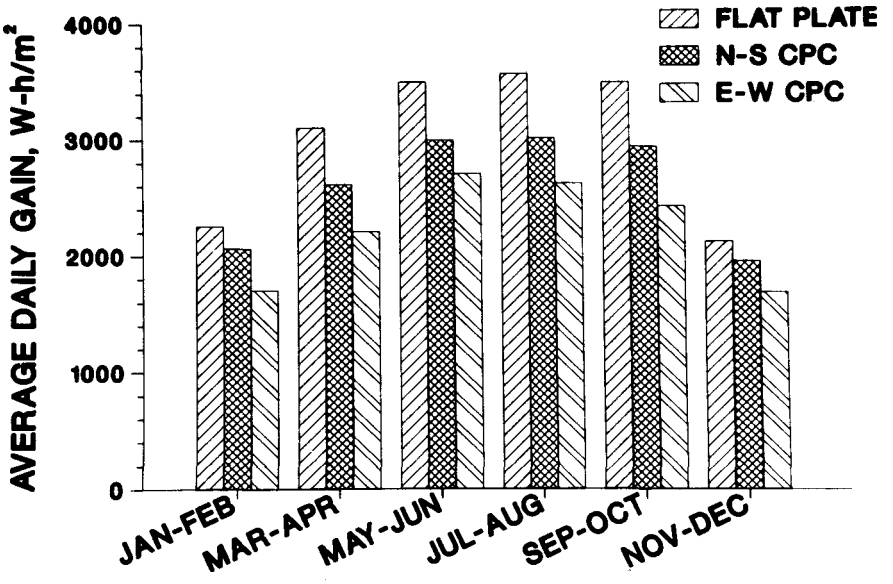

FIGURE 5.5 Simulated Collector Performance at Albuquerque, New Mexico, Based on 1953 Weather Data (Daily starting temperature of storage is 30°C.)

5.1.3 E-W CPC Modifications

We examined some possible reasons for the slightly lower performance of the E-W CPC system at low temperatures by simulating two different modifications to the collector for a daily starting storage temperature of 30°C:

- Removal of the cover glass and
- Rotation of the collector so that the tubes are oriented on an N-S axis, with a tilt angle equal to the latitude.

Figure 5.6 and Table 5.3 allow performance comparisons of (1) the collector as it was operated during the side-by-side tests (i.e., in an E-W orientation and with a cover glass), (2) the same collector in an E-W orientation with the cover glass removed, and (3) the same collector in an N-S orientation and with the cover glass in place.

Removing the cover glass produced a significant (15%) increase in performance, making the E-W CPC virtually as good as the N-S CPC. However, exposing the rather deep troughs of the E-W CPC to the weather could allow them to fill with snow and ice. Moreover, the dust and pollen that could accumulate in an open E-W trough might not be effectively washed out by rain.

Rotation of the E-W CPC so that its tubes were oriented N-S reduced performance slightly. The collector performed less well in this orientation, because its narrow acceptance angle was chosen to favor the E-W orientation.

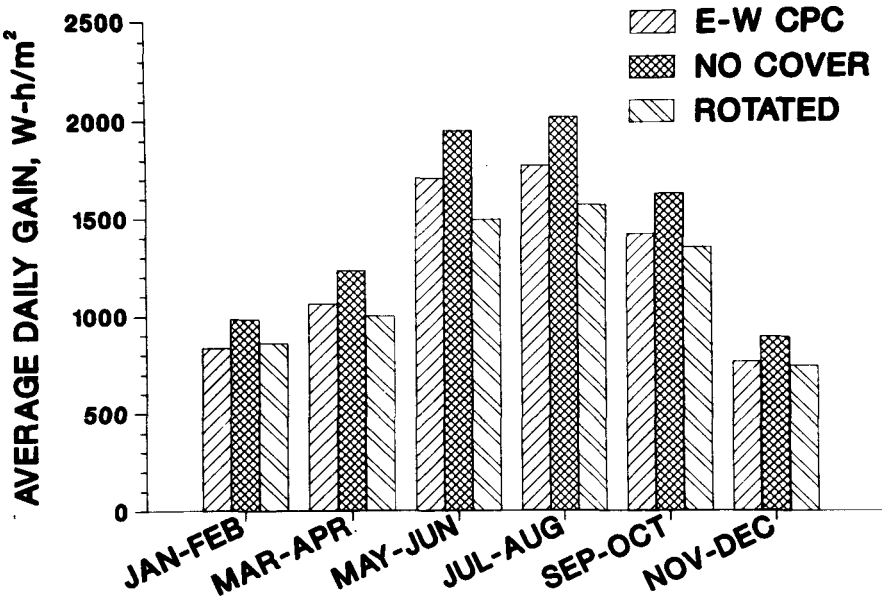

FIGURE 5.6 Effects of Simulated Modifications on E-W CPC Performance at ANL, Based on 1980 Weather Data (Daily starting temperature is 30°C.)

TABLE 5.3 Simulated Modifications of the E-W CPC Collector[a]

Configuration	Energy Delivered Annually by System ($kW \cdot h \cdot m^{-2} \cdot year^{-1}$)	Improvement over Base Design (%)
Base Design	464	---
No Cover Glass	535	15
Collector Rotated to N-S Orientation	431	-7

[a]1980 ANL weather data. Daily starting temperature of storage is 30°C.

5.2 SIMULATED COMPARISONS FOR IMPROVED CPC COLLECTORS AND HIGHER TEMPERATURES

The simulated comparisons descibed in this section involved changes in the optical characteristics of the CPC collectors. Modifying the optical characteristics of the CPC collectors required a simple revision of the parameters of the ray-tracing subroutine used to calculate the optical efficiency. We believe that the model validations of Chapter 4 substantiate the simulations in which the optical characteristics of the CPC collectors were varied.

These comparisons also involved changes in the operating-temperature range of the systems. However, changing the operating-temperature range required detailed knowledge of how the heat-loss coefficients of the collectors vary with operating temperature. Our knowledge of the variations in the heat-loss coefficients with temperature was limited to efficiency curves supplied by the collector manufacturers. Additional tests at higher temperatures would be necessary to fully validate the simulation models at these temperatures. However, we believe the simulation models validated at lower temperatures to be adequate for reasonably accurate relative comparisons of the different systems operated at higher temperatures.

5.2.1 Comparisons Using 1983 State-of-the-Art Collector-Design Improvements

The 1983 state-of-the-art CPC collectors have one design feature that significantly improves their performance with respect to the 1980 state-of-the-art CPC collectors tested at ANL. The manufacturers of both the N-S CPC and the E-W CPC are now using new absorber tubes manufactured by Owens-Illinois, Inc., Toledo, Ohio. The absorptance of the new absorber tubes is about 0.95 (the absorptance of the older tubes was about 0.80); the emittance of the new absorber tubes is 0.06 (the emittance of the old tubes was also 0.06). Techniques for applying a selective absorber surface to glass have only recently improved to the point that absorptance of selective surfaces on commercially available cylindrical glass absorbers is equal in performance to that of selective surfaces on flat metal absorbers.

We have estimated the effects of absorber-tube improvements on system performance by adjusting the absorptance parameters in the ray-tracing subroutine of ANSIM. Figure 5.7 shows comparisons of the average daily gains of the three systems with the 1983 state-of-the-art collectors. The daily starting temperature of the storage tanks was 30°C, and the weather data were for 1980 at ANL. These results can be compared with those of the 1980 state-of-the-art collectors shown in Figure 5.3, which also used a daily starting storage temperature of 30°C and 1980 ANL weather data. The flat plate's performance is the same in both figures, because good flat plate collectors have undergone no major improvements in performance during this period of time. Moreover, flat plate performance has been optimized to the point where little improvement can be expected from current designs in the future. Comparisons of Figure 5.7 with Figure 5.3 show that the performance of the N-S CPC and the E-W CPC has improved to the point where it equals or excells the flat plate collector's performance in most months, even at low temperatures.

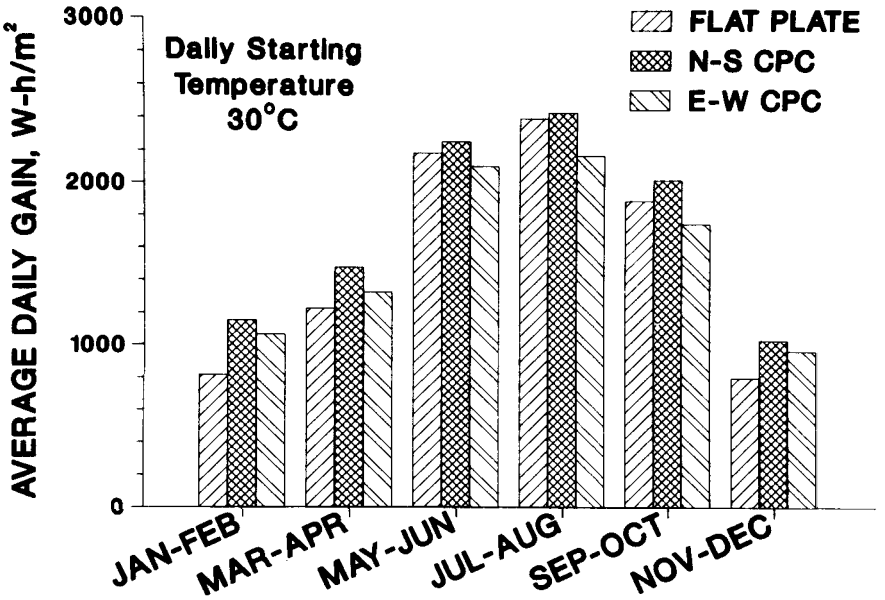

FIGURE 5.7 Simulated System Performance at Low Temperature Using 1983 State-of-the-Art Collectors (The N-S CPC and E-W CPC systems use new, improved absorber tubes, absorptance = 0.95. Daily starting temperature of storage is 30°C. Based on 1980 ANL weather data.)

We stated in Chapter 1 that CPC collector systems are typically operated in a higher temperature range than the 30-60°C range typical of our operating scheme, where the daily starting temperature was 30°C. To examine the effects of higher temperatures on system performance, we have run ANSIM using the 1983 state-of-the-art collectors with daily starting storage temperatures of 75°C and 120°C. Figure 5.8 shows comparisons of system performance for 1983 state-of-the-art collectors with the 75°C daily starting temperature. Figure 5.9 shows comparisons of system performance for the same collectors with the 120°C daily starting temperature. The performance of all three systems decreased with increasing temperature. However, the CPC collectors experienced much less performance degradation at higher temperatures than did the flat plate collector. At these elevated temperatures, the CPC collectors significantly outperformed the flat plate collector. Table 5.4 shows the annual total energy gains for the 1980 state-of-the-art collectors at 30°C daily starting storage temperature and for the 1983 state-of-the-art collectors at 30°C, 75°C, and 120°C daily starting temperatures.

5.2.2 Comparisons of Potential CPC Design Improvements

This section demonstrates the potential for additional improvements in the performance of both E-W and N-S CPCs. The comparisons presented include the CPC absorber-tube improvements (absorptance of 0.95 and emittance of 0.06) that characterize the 1983 state-of-the-art CPC collectors (Section 5.2.1), and improvements in

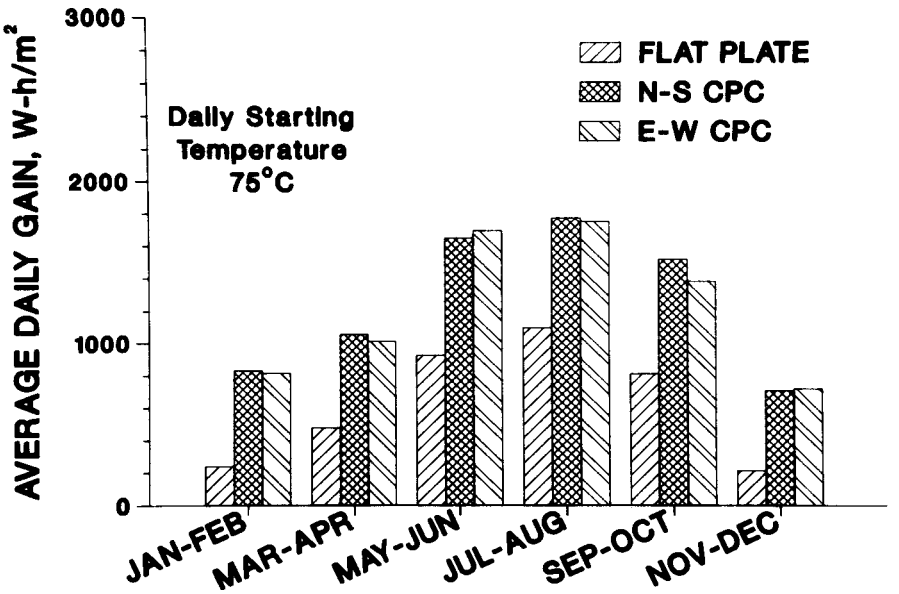

FIGURE 5.8 Simulated System Performance at Higher Temperature Using 1983 State-of-the-Art Collectors (The N-S CPC and E-W CPC systems use new, improved absorber tubes, absorptance = 0.95. Daily starting temperature of storage is 75°C. Based on 1980 ANL weather data.)

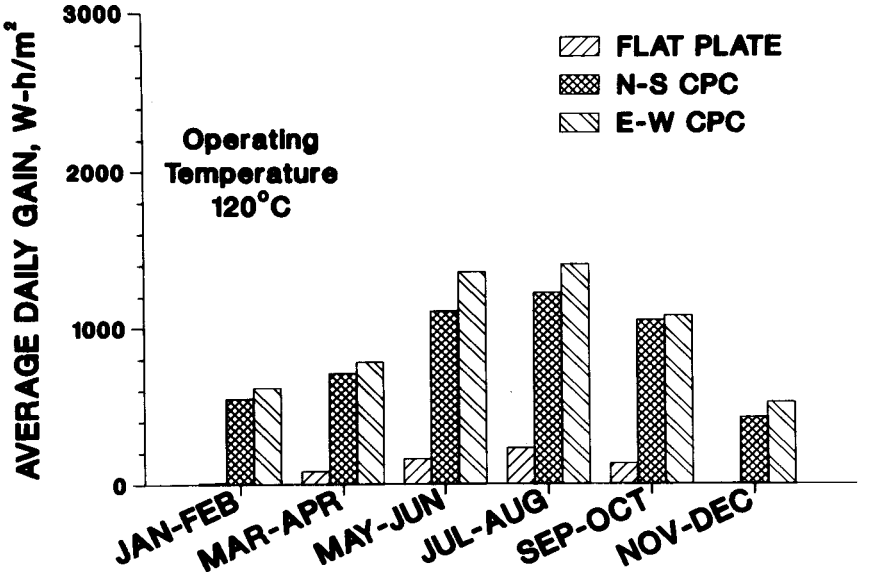

FIGURE 5.9 Simulated System Performance at Steam-Generating Temperature Using 1983 State-of-the-Art Collectors (The N-S CPC and E-W CPC systems use new, improved absorber tubes, absorptance = 0.95. Collector operating temperature is a constant 120°C. Based on 1980 ANL weather data.)

TABLE 5.4 Simulated Comparison of Energy Delivered Annually Using 1980 and 1983 State-of-the-Art Collectors at Three Different Temperatures ($kW \cdot h \cdot m^{-2}$)[a]

	Starting Storage Temperature		Operating Temperature
Collector System	30°C	75°C	120°C
Flat Plate (1980 and 1983)	569	231	38
N-S CPC			
1980	519	353	223
1983	633	461	310
E-W CPC			
1980	464	348	259
1983	573	452	353

[a]1980 ANL weather data.

reflectors are also considered. We have increased the reflectance of the E-W CPC from 0.85 to 0.95 and that of the N-S CPC from 0.80 to 0.95. A silver reflector coating having this reflectance has recently been developed by 3-M Corporation for indoor lighting applications. Over a period of a few months, however, serious deterioration of the coating occurred in an experimental prototype (a sample of the coating exposed to the weather at ANL during the winter of 1982). Thus, further development work is necessary to produce a silver coating that will endure outdoors.

Figure 5.10 presents simulated comparisons using 1980 ANL weather data for five different cases: (1) the current N-S CPC, (2) the N-S CPC with an improved reflector, (3) the N-S CPC with an improved absorber, (4) the N-S CPC with an improved absorber and reflector, and (5) the flat plate system, shown for comparison. In all cases, the daily starting temperature of storage was 30°C. Table 5.5 presents comparisons of annual total energy delivered by the improved N-S CPC collector.

Figure 5.11 presents simulated comparisons using 1980 ANL weather data and 30°C daily starting temperature for six different cases: (1) the current E-W CPC, (2) the E-W CPC with an improved reflector, (3) the E-W CPC with an improved absorber, (4) the E-W CPC with an improved absorber and reflector, (5) the E-W CPC with an improved absorber and reflector and with an anti-reflection cover glass (transmission increased from 0.88 to 0.94), and (6) the flat plate system, shown for comparison. Table 5.6 presents comparisons of annual total energy delivered by the collectors. This table includes an additional case (improved absorber and reflector, no cover glass). The

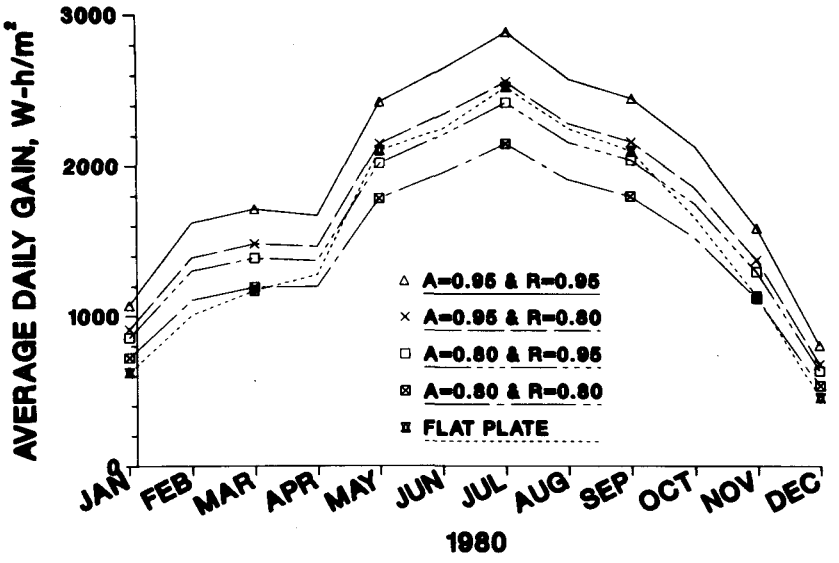

FIGURE 5.10 Effects of Simulated Improvements on N-S CPC Performance (Flat plate performance is shown for comparison. "A" is absorptance, and "R" is reflectance. Daily starting temperature of storage is 30°C. Based on 1980 ANL weather data.)

TABLE 5.5 N-S CPC Improvements: Comparisons of Annual Total Energy Delivered[a]

System	Delivered Energy ($kW \cdot h \cdot m^{-2} \cdot year^{-1}$)	Approach to Best Possible Design Performance (%)
Current N-S CPC Design	519	69
N-S CPC with Improved Reflector	594	79
N-S CPC with Improved Absorber	614	82
N-S CPC with Improved Reflector and Absorber	750	100
Flat Plate	569	--

[a]1980 ANL weather data. Daily starting temperature of storage is 30°C.

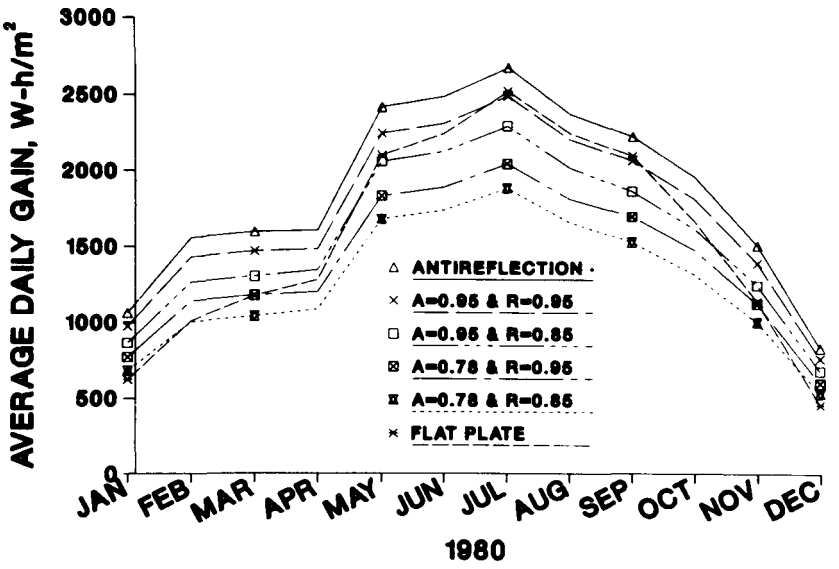

FIGURE 5.11 Effects of Simulated Improvements on E-W CPC Performance (Flat plate performance is shown for comparison. "A" is absorptance, and "R" is reflectance. Daily starting temperature of storage is 30°C. Based on 1980 ANL weather data.)

performance of the E-W CPC without a cover glass is just slightly less than that of the N-S CPC, as would be expected. (The E-W CPC has a smaller acceptance angle, and therefore sees less diffuse radiation, than does the N-S CPC.)

We conclude that there is great potential for increasing the performance of CPC collectors. Improving the absorber elevated the performance so that both CPCs at ANL outperformed a well-built flat plate, even at low temperatures. The best possible designs produced a very substantial (44 to 47%) increase in performance at low temperatures over current CPC designs. At steam-generating temperatures (120°C), the increase in performance was 79 to 87%.

5.2.3 Comparisons for Steam-Generating Temperatures

The daily operating temperatures that occur with an initial daily storage temperature of 30°C are not representative of several solar heating-system applications, such as industrial low-pressure steam production, absorption air conditioning, or advanced low-temperature Rankine-cycle air conditioning. We have simulated operation of the three systems with the collectors operating at a constant 120°C each day. This condition would be experienced when generating steam at 15 psig.

Figure 5.12 presents simulated comparisons of the average daily gain each month by the collectors operating at a constant 120°C, based on 1980 ANL weather data. Table 5.7 presents simulated comparisons of the total energy delivered by the collectors when

TABLE 5.6 E-W CPC Improvements: Comparisons of Annual Total Energy Delivered[a]

System	Delivered Energy ($kW \cdot h \cdot m^{-2} \cdot year^{-1}$)	Approach to Best Possible Design Performance (%)
Current E-W CPC Design	464	68
E-W CPC with Improved Reflector	514	75
E-W CPC with Improved Absorber	572	84
E-W CPC with Improved Reflector and Absorber	632	92
E-W CPC with Improved Reflector and Absorber and Anti-Reflection Glass	684	100
E-W CPC with Improved Reflector and Absorber and No Cover Glass	732	--[b]
Flat Plate	569	

[a]1980 ANL weather data. Daily starting temperature of storage is 30°C.

[b]This collector requires a cover glass.

operating at this temperature. The standard CPC collectors were the 1980 state-of-the-art collectors. The improved E-W CPC had a coating with an absorptance of 0.95 and an emittance of 0.05, a concentrator with a reflectance of 0.95, and a cover glass with a transmissivity of 0.94. The improved N-S CPC had a coating with an absorptance of 0.95 and an emittance of 0.05 and had a mirror with a reflectance of 0.95. The rankings of the three systems according to the performance estimates at 120°C are reversed from the rankings at 30°C. At the lower temperature, the E-W CPC had the poorest performance, because it had the lowest optical efficiency. At the higher temperature, the E-W CPC had the best performance, because it had the lowest heat-loss coefficient. This result would be expected, because the E-W CPC was designed for higher-temperature operation.

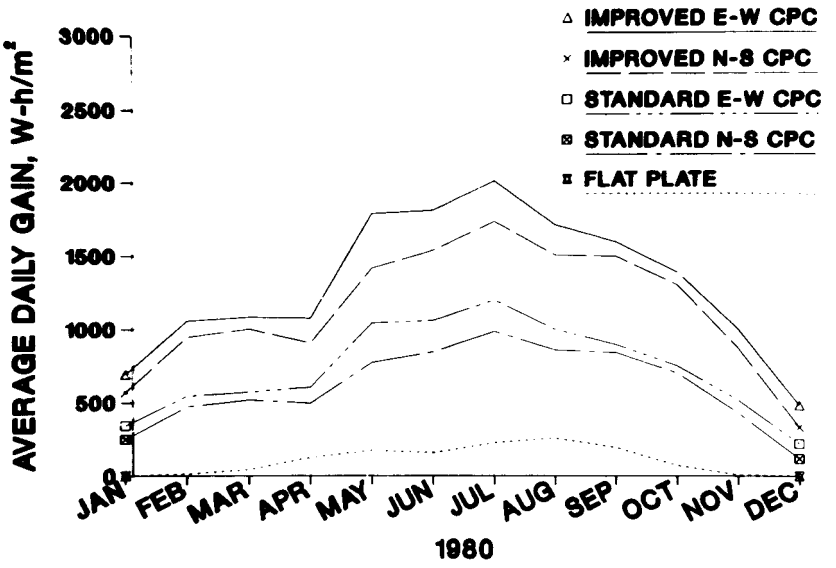

FIGURE 5.12 Simulated Comparisons at 15-psig Steam-Generating Temperature (120°C)

TABLE 5.7 Comparisons of Simulated Energy Delivered Annually at Constant 120°C[a]

System	Delivered Energy ($kW \cdot h \cdot m^{-2} \cdot year^{-1}$)
Improved E-W CPC	480
Improved N-S CPC	417
Standard E-W CPC	268
Standard N-S CPC	223
Flat Plate	39

[a]1980 ANL weather data. See Section 5.2.3 for description of standard and improved CPC collectors.

Finally, we have summarized the effects that changes in the collector operating-temperature range have on system performance. Table 5.8 shows the decrease in annual total energy delivered caused by increasing the starting temperature from 30°C to 120°C.

TABLE 5.8 Decrease in Simulated Energy Delivered Annually Caused by Increasing the Starting Temperature from 30°C to 120°C[a]

System	Simulated Energy Delivered ($kW \cdot h \cdot m^{-2} \cdot year^{-1}$)		Energy Decrease (%)
	30°C Starting Temperature	120°C Starting Temperature	
E-W CPC			
Improved	684	480	30
Standard	464	268	42
N-S CPC			
Improved	750	417	44
Standard	519	223	57
Flat Plate	569	39	93

[a]1980 ANL weather data. See Section 5.2.3 for description of standard and improved CPC collectors.

6 SYSTEM TESTING AND RATING METHODS

In this chapter, we evaluate proposed solar-heating-system testing and rating methods in the light of our measured and simulated results. The need for a method of testing complete systems is becoming widely recognized among professional solar-energy designers and engineers. It is difficult to obtain test results that can be used to rate the performance of a system, because a system's operating conditions vary widely over the course of a year. Operating conditions that vary to a considerable degree include temperature (in storage, in the collector loop, and outdoors), solar radiation (beam, sky, and ground components), wind speed, and precipitation (rain, snow, and ice).

The most conclusive kind of system test would be operation of an instrumented system for one year or longer. However, such tests require considerable time and expense, so that they would be appropriate only for performing general comparisons of different generic systems. Also, the applicability of such test results is limited to geographic locations with climates similar to the climate of the test location.

The solar-energy industry needs (1) a system-testing procedure that produces in a short time and at moderate expense a system rating applicable to a particular geographic region and (2) a method of extending the rating to other regions.

This chapter discusses three different options for system testing and rating:

- Indoor testing (ASHRAE Standard 95-1981);[4]
- Short-term, outdoor side-by-side tests with a reference system (the relative solar rating method);[5] and
- A combination of short-term system tests with simulation modeling.

6.1 INDOOR TESTING

In February 1977, the American Society of Heating, Refrigeration, and Air-Conditioning Engineers formed Standards Project Committee 95-P to develop a standard test method for solar domestic-hot-water (SDHW) systems.

Two indoor testing procedures were developed and incorporated into ASHRAE Standard 95-1981.[4] One procedure uses a solar simulator lamp as a source of radiant energy in place of solar radiation. The other procedure uses a nonirradiated collector array in series with an electric resistance heater. The heater is manually controlled so that the output of the collector-heater combination simulates the output of an irradiated collector.

The procedure using the solar simulator lamp requires no prior tests of system components, whereas the procedure using the collector-heater combination requires prior tests of the collector. These tests are necessary to determine the collector's thermal-loss coefficient and its optical efficiency at various incidence angles.

The use of a solar simulator lamp presents several problems that diminish the usefulness of the test procedure. Apparatus for mounting and moving the lamp throughout the day so that it mimics the motion of the sun is complex and expensive, especially when large arrays must be irradiated. Also, it is difficult, if not impossible, to simulate the correct proportions of beam, sky, and diffuse radiation. These considerations are especially important when CPC collectors are tested, because of these collectors' unusual and varied optical responses.

The procedure using the nonirradiated collector in series with an electric resistance heater is easier to implement. However, little new information is obtained from the test. The amount of energy delivered to the system by the electric resistance heater is calculated from previously determined collector parameters. The nonirradiated collector is included so that collector heat capacity and system controller operation are adequately represented. However, it has been shown that excellent agreement between actual outdoor performance and simulated indoor performance can be obtained by using an electric resistance heater alone in place of the irradiated collector.[4]

Another proposed indoor testing procedure, which has not yet been incorporated into an ASHRAE standard, requires only that the optical parameters from prior collector tests be known. However, this method necessitates disassembly of the collector and fastening of electric strip heaters to its back to serve as the heat source.[4] Some collector designs, including many evacuated-tube designs, cannot be disassembled for such testing.

Ideally, a system-testing procedure should yield all of the information necessary for system rating without requiring prior testing of components. This objective can be very difficult to achieve with an indoor testing procedure.

6.2 SHORT-TERM OUTDOOR TESTING

Outdoor testing eliminates the difficulties associated with solar simulator lamps and electric collector simulators. However, much control over testing conditions is relinquished to the random nature of the weather.

One proposed method of short-term outdoor testing is the relative solar rating method.[5] This procedure calls for the operation of a test system and a reference system side-by-side for a single day. The long-term performance of the reference system is known through monitoring or simulation. The test yields useful information only if the ratio of the daily solar fractions of the test and reference systems is uniquely related to the corresponding annual ratio.

Chandra and Khattar[5] have explored the validity of this method by simulating the side-by-side performance of test systems and baseline systems that use flat plate collectors. They have concluded that in sunny, warm climates that experience little seasonal variation in weather (Miami, Florida; Santa Maria, California; and Phoenix, Arizona), the daily performance ratio is closely related to the annual performance ratio for nearly 80% of the days of a typical meteorological year. However, such a relationship cannot be found for Boston, Massachusetts, which has a typical northern climate and experiences substantial weather variations throughout the year.

The results of the side-by-side testing and computer modeling done at ANL confirm that the relative solar rating method is not generally applicable to climates with substantial weather variations or to comparisons of systems with collectors that have significantly different optical and thermal performance characteristics.

On clear summer days, the flat plate system performs better than the CPC systems. However, on a cloudy summer day or on most winter days, the CPC systems perform better than the flat plate system. On most days, the N-S CPC performs better than the E-W CPC, but the ratio of the daily energy gains of the two systems varies substantially from day to day.

6.3 COMBINATION OF SHORT-TERM OUTDOOR TESTING AND SIMULATION MODELING

Short-term outdoor tests need not be limited to single-day tests. One or two weeks of operation may be adequate to characterize the performance of a system during a particular season. Furthermore, our results from operations conducted with a daily starting storage temperature of 50°C suggest that some features of winter performance can be obtained by operating a system at higher temperatures during the summer. Comparisons of simulated system performance with measured performance suggest that systems can be rated by using a validated computer simulation model.

Short-term outdoor tests that force the system to function in different operating modes over a range of operating temperatures can very likely be combined with a computer simulation model to produce valid system ratings for different climates. Balon and Wood[15] have recently proposed correlating an estimate of system performance with indoor test results using the nonirradiated-collector procedure of ASHRAE Standard 95-1981.[4] However, the estimate is based on the f-Chart (Version 4.0) computer program, so that the analysis is limited to the types and sizes of systems that can be handled by the f-Chart regression formula.

Further research is necessary to identify a set of parameters obtainable from a short-term system test and capable of fully characterizing the system. The usefulness of such parameters depends on the existence of a "universal system model" that can incorporate the parameters and produce system performance results. A universal system model is analogous to the Hottel-Whillier-Bliss equation with incidence-angle modifiers, which serves as a "universal collector model" applicable to almost any collector.

Solar collectors can be modeled by developing theoretical descriptions of each collector component, such as glazing, absorber plate, insulation, etc. In the modeling of different collector designs, a different set of parameters -- glazing transmittance, absorber-plate absorptance and emittance, insulation conductivity, etc. -- is required for each collector modeled. System simulation models (such as ANSIM or TRNSYS) are analogous to highly detailed collector models. However, there is currently no system analog to the Hottel-Whillier-Bliss equation for collectors. This equation characterizes a collector by means of only two parameters ($F_R\eta_o$ and F_RU_L), which are determined by short-term tests.

The system parameters presented in Section 3.3 represent a first step in the search for parameters usable in a universal model. Furthermore, the ANSIM model provides a framework that may be extended to develop a universal model that requires a minimum of computing time, can be implemented on small computers, and has sufficient flexibility to cover a large number of different system designs.

We recommend that consideration be given to developing a standard for collector-system testing that incorporates testing for a small number of days at two or more temperatures and then using the resulting data as input to a "universal" solar-heating-system computer simulation model capable of predicting system performance.

REFERENCES

1. Winston, R., and H. Hinterberger, *Principles of Cylindrical Concentrators for Solar Energy*, Solar Energy *17*:255-258 (1975).

2. Collares-Pereira, M., et al., *Design and Performance Characteristics of Compound Parabolic Concentrators with Evacuated and Non-evacuated Receivers*, Proc. of the International Conf. on Solar Energy *2*:1295, Atlanta, Ga. (1979).

3. Klein, S.A., W.A. Beckman, and J.A. Duffie, *A Design Procedure for Solar Heating Systems*, Solar Energy *18*:113 (1976).

4. Fanney, A.H., W.C. Thomas, C.A. Scarbrough, and C.P. Terlizzi, *Analytical and Experimental Analysis of Procedures for Testing Solar Domestic Hot Water Systems*, National Bureau of Standards Science Series 140 (1982).

5. Chandra, S., and M.K. Khattar, *Analytical Investigations of the Relative Solar Rating Concept*, Draft Final Report, Florida Solar Energy Center (June 1980).

6. Fanney, A.H., and S.T. Liu, *Comparison of Experimental and Computer Predicted Performance for Six Solar Domestic Hot Water Systems*, ASHRAE Transactions *86*(1):823-835 (1984).

7. McIntire, W., and K. Reed, *Incident Angle Modifiers for Evacuated Tube Collectors*, Proc. of the American Section of the International Solar Energy Society, Inc., Solar Rising, Philadelphia, Penn., p. 282 (1981).

8. McGarity, A.E., C.S. ReVelle, and J.L. Cohon, *Analytical Simulation Models for Solar Heating System Design*, Solar Energy *32*(1):85 (1984).

9. Boes, E.C., et al., *Distribution of Direct and Total Solar Radiation Availabilities for the USA*, Sandia National Laboratory Report SAND-76-0411, Albuquerque, N.M. (Aug. 1976).

10. Klein, S.A., et al., *A Method of Simulation of Solar Processes and its Application*, Solar Energy *17*:39 (1975).

11. *Data Requirements and Thermal Performance Evaluation Procedures for Solar Heating and Cooling Systems*, Task I Report, International Energy Agency, Solar R and D Program, NTIS (Aug. 1979).

12. Duffie, J.A., and W.A. Beckman, *Solar Engineering of Thermal Processes*, John Wiley and Sons, New York (1981).

13. *Methods of Testing to Determine the Performance of Solar Collectors*, American Society of Heating, Refrigeration, and Air-Conditioning Engineers, ASHRAE Standard 93-77 (Feb. 1977).

14. *Hourly Solar Radiation-Surface Meteorological Observations,* SOLMET Final Report TD-9724, National Oceanic and Atmospheric Administration (U.S. Department of Commerce), Asheville, N.C. (Feb. 1979).

15. Balon, R.J., and B.D. Wood, *Performance Testing and Rating of Commercial Solar Domestic Hot Water Systems,* Proc. of the American Solar Energy Society, Progress in Solar Energy 5:431 (June 1982).

INITIALISMS

ANL	Argonne National Laboratory
ANSIM	Analytical simulation
ASHRAE	American Society of Heating, Refrigeration, and Air-Conditioning Engineers
CPC	Compound parabolic concentrator
D-ANSIM	Daily analytical simulation
DHW	Domestic hot water
DOE	U.S. Department of Energy
E-W	East-west
L-ANSIM	Linear (hourly) analytical simulation
NBS	National Bureau of Standards
N-S	North-south
PSP	Precision Spectral Pyranometer
SDHW	Solar domestic hot water
VMS	Virtual-memory operating system
ZV	Zone heating valve

Distribution for ANL-82-81

Internal:

J.G. Asbury
J.W. Allen (51)
F.C. Bennett
L. Burris (2)
R.L. Cole
E.J. Croke
J.J. Dzingel
A.J. Gorski
J.R. Hull
A.B. Krisciunas
K.S. Macal
A.I. Michaels
J.E. Parks
J.J. Roberts
W.W. Schertz (50)
A.S. Wantroba
ANL Patent Office
ANL Contract File
ANL Libraries
TIS File (6)

External:

DOE-TIC for distribution per UC-59a (327)
Manager, Chicago Operations Office, DOE-CH
Chemical Technology Division Review Committee
S. Baron, Burns and Roe, Inc., Oradell, N.J.
W.N. Delgass, Purdue University
K.H. Keller, University of Minnesota, Minneapolis
T.A. Milne, Solar Energy Research Institute, Golden, Colo.
H. Perry, Resources for the Future, Washington, D.C.
R. Winston, Enrico Fermi Institute, The University of Chicago
W.L. Worrell, University of Pennsylvania, Philadelphia
E.B. Yeager, Case Western Reserve University
Air Conditioning and Refrigeration Institute, Arlington, Va.
P. Ambrosetti, Swiss Federal Institute for Reactor Research, Wurenlingen, Switzerland
H.E.B. Andersson, Swedish Council for Building Research, Stockholm
E. Aranovitch, European Joint Commission, Euratom Research Center, Ispra, Italy
G. Austin, Commonwealth Edison Co., Chicago
J.D. Balcomb, Los Alamos Scientific Laboratory, N.M.
C.A. Bankston, Washington, D.C.
A. Barak, National Council for Research, Tel Aviv, Israel
W. Beckman, University of Wisconsin, Madison
R.F. Benseman, Department of Scientific and Industrial Research,
Lower Hutt, New Zealand
C. Boussemaere, Polytechnic Institute of Mons, Belgium
D.S. Breger, Allston, Mass.
B. Brinkworth, University College, Cardiff, U.K.
M. Bruck, Austrian Solar and Space Agency, Vienna
E. Buyco, University of Petroleum and Minerals, Dhahran, Saudi Arabia
M. Collares-Pereira, Center for the Physics of Materials, Lisbon, Portugal
J.D. Connelly, Energy Design Corp., Memphis, Tenn.
C. Conner, U.S. Department of Energy, Washington, D.C.
J. Dalenback, Chalmers University of Technology, Gothenburg, Sweden
C. den Ouden, Institute of Applied Physics, Delft, The Netherlands

DSET Laboratories, Inc., Phoenix, Ariz.
J.A. Duffie, University of Wisconsin, Madison
G. Ford, Energy Design Corp., Memphis, Tenn.
E. Francis, Illinois State University
J. Frissora, Sunmaster Corp., Corning, N.Y.
R. Fu-Min, Chinese Assn. of Refrigeration, Beijing, China
K. Fuller, New York State Electric and Gas Co., Binghamton, N.Y.
J.D. Garrison, San Diego State University, Calif.
S.J. Harrison, National Research Council of Canada, Ottawa, Ontario
A. Heitz, Lawrence Berkeley Laboratory, University of California, Berkeley
H. Hinterberger, Fermilab, Batavia, Ill.
D. Hsieh, University of Florida, Gainesville
J. Keller, Swiss Federal Institute for Reactor Research, Wurenlingen, Switzerland
N. Kenny, Corning Glass Works, Corning, N.Y.
M.-I. Lee, Energy Research Laboratory, ITRI, Taipei, Taiwan, Republic of China
G.O.G. Lof, Colorado State University, Fort Collins
N.A. Mancini, Institute of Physics, University of Catania, Italy
J. Martin, Gosport, Ind.
G. Mather, Owens-Illinois, Inc., Toledo, Ohio
A.E. McGarity, Swarthmore College, Penn. (50)
W. McIntire, Tulsa, Okla.
E. Mezquida, National Institute of Aerospace Technology, Madrid, Spain
E. Morofsky, Public Works Canada, Ottawa, Ontario
F. Morse, U.S. Department of Energy, Washington, D.C.
J.J. O'Gallagher, Enrico Fermi Institute, The University of Chicago
P.V. Pedersen, Thermal Insulation Laboratory, Technical University of Denmark, Lyngby
M. Platt, Sunmaster Corp., Corning, N.Y.
D. Proctor, CSIRO, Highett, Victoria, Australia
A. Rabl, Princeton University
E. Ramos, University of Mexico, Mexico City
K. Reed, National Bureau of Standards, Washington, D.C.
A. Remnitz, Solar Rating and Certification Corp., Washington, D.C.
I. Rickling, Florida Solar Energy Center, Cape Canaveral, Fla.
W. Scholkopf, University of Munich, Federal Republic of Germany
S. Schweitzer, U.S. Department of Energy, Washington, D.C.
R. Shibley, Anchorage, Alaska
L. Spanoudis, Owens-Illinois, Inc., Toledo, Ohio
H.J. Stein, Solar Energy Branch/IKP, Nuclear Energy Research Establishment, Julich, Federal Republic of Germany
D. Stipanuk, Cornell University
J.M. Suter, Swiss Federal Institute for Reactor Research, Wurenlingen, Switzerland
S. Svendsen, Thermal Insulation Laboratory, Technical University of Denmark, Lyngby
C.J. Swet, Mt. Airy, Md.
H. Tabor, National Physical Laboratory of Israel, Jerusalem
H.D. Talarek, Solar Energy Branch/IKP, Nuclear Energy Research Establishment, Julich, Federal Republic of Germany
S. Tanemura, Government Industry Research Institute, Nagoya, Japan
G. Thodos, Northwestern University, Evanston, Ill.

W. Thomas, Virginia Polytechnic Institute and State University
V. Ussing, Thermal Insulation Laboratory, Technical University of Denmark, Lyngby
D. Vine, Tennessee Valley Authority, Chattanooga
L. Wei-De, Beijing Solar Energy Research Institute, Beijing, China
H. Wennerholm, National Testing Institute, Boras, Sweden
H. Wenzel, TUV Bavaria, Munich, Federal Republic of Germany
A.J.T.M. Wijsman, Institute of Applied Physics, Delft, The Netherlands
B. Wood, Arizona State University, Tempe
M. Yarosh, Florida Solar Energy Center, Cape Canaveral, Fla.

The final chapter of this report evaluates proposed solar-heating-system testing and rating methods in light of our measured and simulated results. A combination of short-term tests (one to two weeks) and simulation modeling is suggested as a system rating method.